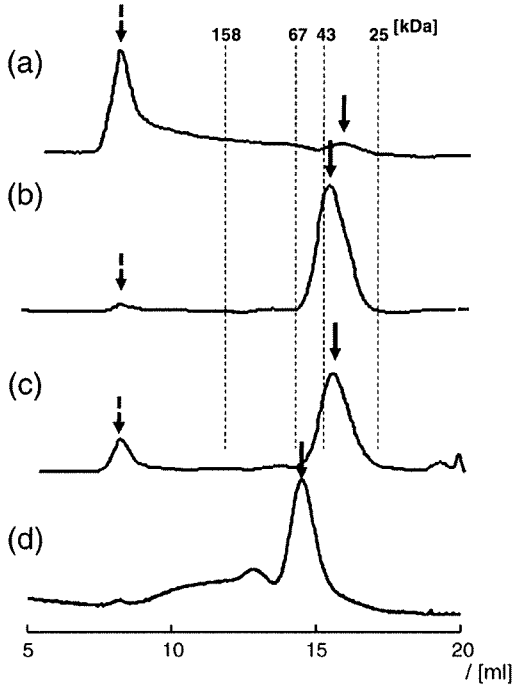

FIG. 4. Gel filtration chromatography results for (a) untreated scFv-cys, (b) scFv-cys PEGylated with mPEG-5 after refolding, (c) scFv-cys PEGylated with mPEG-5 during refolding, and (d) untreated and partially refolded scFv-cys in 0.4 M L-arginine. The fractions indicated by solid and broken arrows correspond to a monomeric form and highly multimeric forms of scFv-cys, respectively. The elution buffers used for (a)–(c) were PBS solution, and the buffer for (d) was PBS solution containing 0.4 M L-arginine.

In the case of PEGylation with mPEG-20, the conjugation reaction also transformed the highly multimeric forms to several forms with smaller sizes (solid arrows in Fig. 5); however, residual highly multimeric forms were observed in the chromatograms of the scFv-cys fragments PEGylated both after refolding and during refolding (broken arrows in Fig. 5). When we conducted SDS-PAGE and Western blotting analysis of the fractions, the fraction containing the residual highly multimeric forms contained both PEGylated and non-PEGylated scFv-cys fragments, whereas other fractions (broken arrows in Fig. 5) contained only PEGylated scFv-cys (data not shown). This result implies that the low efficiency of chemical conjugation for mPEG-20 resulted in less transition to a monomeric form and less suppression of aggregation during the refolding process.

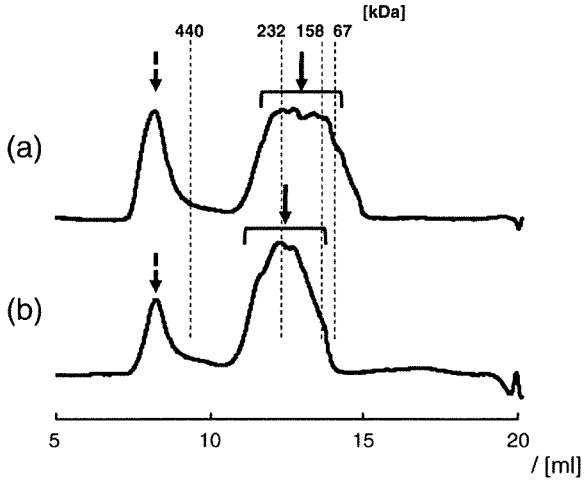

FIG. 5. Gel filtration chromatography results for (a) scFv-cys PEGylated with mPEG-20 after refolding and (b) scFv-cys PEGylated with mPEG-20 during refolding. The fractions indicated by solid arrows correspond to scFv-cys formed by PEGylation, and the fraction indicated by broken arrows corresponds to highly multimeric forms of scFv-cys, respectively.

Flow cytometric analysis of antigen binding activity of pegylated 528 scFv The binding affinity of PEGylated scFv-cys fragments for A431 cells of a human epidermoid cancer cell line was measured by means of flow cytometry to confirm the activity of PEGylated scFv-cys (Fig. 6). The flow cytometry results for PEGylation with mPEG-5 showed that the scFv-cys fragments PEGylated after refolding and those PEGylated during refolding had binding activity for the EGFR antigen (Fig. 6a), and similar results were observed for the PEGylation with mPEG-20 (Fig. 6b). These results indicate that the combination of refolding and site-specific PEGylation can be used to prepare active PEGylated scFv fragments from insoluble aggregates.

DISCUSSION

Advances in antibody engineering have enabled the construction of tailor-made therapeutic antibodies by means of the artificial buildup from immunoglobulin domains, including scFv fragments (23), tandem scFv fragments (24), diabodies (25), single-chain diabodies (26), and minibodies (27). These recombinant compact antibodies can potentially be mass produced in *E. coli* expression systems at low cost, and site-specific PEGylation of these compact antibodies can overcome one of their disadvantages—their rapid elimination from the body (28). However, in most cases, compact antibodies are expressed in *E. coli* systems as insoluble aggregates of proteins (10, 11), and refolding is not always efficient enough, because of the reagglomeration to soluble and insoluble aggregates.

We found here that PEGylation of a cysteine-substituted h528 scFv fragment promoted the conversion of soluble aggregates to monomeric forms, and this result shows that this method is promising for use in drug formulation. Although h528 scFv can be refolded from insoluble aggregates (15), the addition of the cysteine residue at the C-terminus of the VH domain led to the misfolding of scFv-cys into multimeric forms in the refolding process; however, PEGylation with mPEG-5 after refolding transformed the soluble aggregates to active monomeric forms (Fig. 4). PEGylation after refolding led to a transition from highly multimeric forms to a monomeric form. In order to analyze the formation of intermolecular disulfide linkage in the multimeric forms, we measured the SDS-PAGE of multimeric forms in nonreducing conditions; consequently, several multimeric forms of scFv via intermolecular disulfide linkage were observed. This result suggests that the reduction process in the PEGylation process break the unfavorable disulfide linkage and that the PEGylation on thiol groups suppressed the reformation of intermolecular disulfide linkage and increased the solubility of scFv. We consider that the conversion to a monomeric form by PEGylation occurred because of the increase in solubility afforded by conjugation with PEG molecules.

The chemical efficiency of PEGylation was improved by the use of a small PEG molecule and partially refolded scFv-cys (Fig. 3). The fact that the partially refolded scFv-cys was monomeric in the 0.4 M L-arginine refolding solution indicates that the chemical conjugation efficiency of the refolding-coupled PEGylation depended on the molecular mobility of the PEG and the protein: small PEG molecules associated easily with the thiol group in h528scFv-cys, and the monomeric form of partially refolded scFv-cys had more opportunities to approach the maleimide group of mPEG than did the multimeric forms that were present after refolding. In addition, the PEGylation efficiency influenced the conversion from highly multimeric forms to a monomeric form (Scheme I) and led to suppression

Please cite this article as: Kumagai, I., et al., Integration of PEGylation and refolding for renaturation of recombinant proteins from insoluble aggregates produced in bacteria–Application to a single-chain Fv fragment, J. Biosci. Bioeng. (2009), doi:10.1016/j.jbiosc.2009.10.016

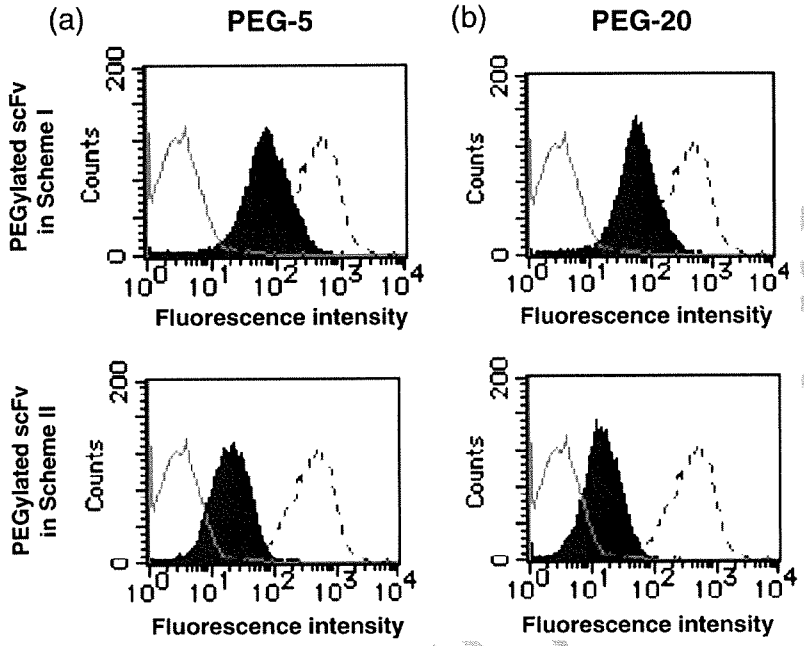

FIG. 6. Flow cytometry analysis of the binding affinity of scFv-cys PEGylated (a) with mPEG-5 and (b) with mPEG-20, for A431 cells. Open and filled areas correspond to the signals from A431 cells incubated without antibodies and cells incubated with PEGylated scFv-cys, respectively. The area indicated by dashed line corresponds to the signals from A431 cells incubated with h528 IgG antibodies.

of the formation of the soluble aggregates (Scheme II). This result suggests that residual unreacted scFv induced PEGylated scFv to form the soluble aggregates. The improvement of PEGylation efficiency might be important for the mass production of scFv conjugated with high-molecular-weight PEG from insoluble aggregates produced in *E. coli*.

The VH and VL domains of Fv have an internal disulfide linkage that is of particular importance for the stability of the immunoglobulin fold (9, 29). L-Arginine has been used in many refolding systems to suppress protein aggregation by inhibiting hydrophobic interactions between protein surfaces (30-32), and our previous study indicated that scFv forms native secondary and tertiary structures in 0.4 M L-arginine solution (14). In this study, PEGylation resulted in the predominant production of scFv conjugated with one mPEG molecule (Fig. 3), and the activity analysis showed that the activity of the refolded and PEGylated scFv was comparable to that of the unmodified scFv reported previously (15). The formation of a partially refolded intermediate might have inhibited the reaction between the maleimide group of mPEG and the cysteine residues involved in the internal disulfide linkages in scFv. In the SDS–PAGE results (Fig. 3), we observed heterogeneous fractions with molecular weights higher than that of scFv-cys conjugated with one mPEG molecule. We are currently conducting a structural analysis using mass spectrometry to improve the control of PEGylation during the refolding process.

The scFvs PEGylated after refolding (Scheme I) had 10–50-fold lower binding activity than that of IgG-type antibodies due to the decrease of valence (Fig. 6). However, when we compared the activity of the scFv PEGylated after refolding with that of previously measured normal scFv (without the fusion of Cys) on the basis of the comparison with the activity of IgG (Kumagai et al., unpublished data), the PEGylated scFv fragments had comparable activity to that of normal scFv. This indicates that the PEGylated scFv fragments in Scheme I have almost full antigen activity. In the case of scFv PEGylated during refolding (Scheme II), the binding activity of the PEGylated scFv was lower than that of PEGylated scFv in Scheme I. Considering that PEGylation yield was increased in Scheme II, this fact might imply that PEGylation during refolding lead to the increase of monomeric PEGylated scFv fragments but that some monomeric forms have no binding activity.

Recently, we reported that the VH and VL domains of anti-EGFR monoclonal antibody 528 are effective for cancer immunotherapy, and we constructed a humanized functional bispecific diabody, hEx3, retargeting T-LAK against an EGFR-positive cell line (15, 33). hEx3 was produced in a refolding system from aggregated forms expressed in *E. coli*. The PEGylation-integrated refolding system described in this report should be useful for improving the yield, molecular properties, and pharmacokinetics in vivo of the hEx3 diabody, as well as other related proteins, such as a tandem scFv fragments and single-chain diabodies.

In conclusion, we obtained an active site-specifically PEGylated scFv fragment from insoluble fractions expressed in *E. coli* by integrating PEGylation and refolding. PEGylation after refolding promoted the conversion of soluble aggregates to monomeric structures, and PEGylation during refolding increased the chemical conjugation efficiency owing to increased molecular mobility. Integration of PEGylation and refolding should be useful for efficient production of PEGylated compact antibodies using *E. coli* expression.

ACKNOWLEDGMENTS

This work was supported by the Japan Science and Technology Corporation (2005 to I.K.) and the Ministry of Education, Culture, Sports, Science and Technology (20015004 to I.K.).

References

1. **Anand, N. N., Mandal, S., MacKenzie, C. R., Sadowska, J., Sigurskjold, B., Young, N. M., Bundle, D. R., and Narang, S. A.:** Bacterial expression and secretion of various single-chain Fv genes encoding proteins specific for a Salmonella serotype B O-antigen, J. Biol. Chem., **266**, 21874–21879 (1991).

Please cite this article as: Kumagai, I., et al., Integration of PEGylation and refolding for renaturation of recombinant proteins from insoluble aggregates produced in bacteria—Application to a single-chain Fv fragment, J. Biosci. Bioeng. (2009), doi:10.1016/j.jbiosc.2009.10.016

2. **Venturi, M., Seifert, C., and Hunte, C.:** High level production of functional antibody Fab fragments in an oxidizing bacterial cytoplasm, J. Mol. Biol., **315**, 1–8 (2002).
3. **Holliger, P. and Hudson, P. J.:** Engineered antibody fragments and the rise of single domains, Nat. Biotechnol., **23**, 1126–1136 (2005).
4. **Chapman, A. P.:** PEGylated antibodies and antibody fragments for improved therapy: a review, Adv. Drug Deliv. Rev., **54**, 531–545 (2002).
5. **Weir, A. N., Nesbitt, A., Chapman, A. P., Popplewell, A. G., Antoniw, P., and Lawson, A. D.:** Formatting antibody fragments to mediate specific therapeutic functions, Biochem. Soc. Trans., **30**, 512–516 (2002).
6. **Bailon, P., Palleroni, A., Schaffer, C. A., Spence, C. L., Fung, W. J., Porter, J. E., Ehrlich, G. K., Pan, W., Xu, Z. X., and Modi, M. W., et al.:** Rational design of a potent, long-lasting form of interferon: a 40 kDa branched polyethylene glycol-conjugated interferon alpha-2a for the treatment of hepatitis C, Bioconjug. Chem., **12**, 195–202 (2001).
7. **Greenwald, R. B., Choe, Y. H., McGuire, J., and Conover, C. D.:** Effective drug delivery by PEGylated drug conjugates, Adv. Drug Deliv. Rev., **55**, 217–250 (2003).
8. **Kubetzko, S., Sarkar, C. A., and Pluckthun, A.:** Protein PEGylation decreases observed target association rates via a dual blocking mechanism, Mol. Pharmacol., **68**, 1439–1454 (2005).
9. **Glockshuber, R., Schmidt, T., and Pluckthun, A.:** The disulfide bonds in antibody variable domains: effects on stability, folding in vitro, and functional expression in *Escherichia coli*, Biochemistry, **31**, 1270–1279 (1992).
10. **Field, H., Yarranton, G. T., and Rees, A. R.:** Expression of mouse immunoglobulin light and heavy chain variable regions in *Escherichia coli* and reconstitution of antigen-binding activity, Protein Eng, **3**, 641–647 (1990).
11. **Pluckthun, A.:** Mono- and bivalent antibody fragments produced in *Escherichia coli*: engineering, folding and antigen binding, Immunol. Rev., **130**, 151–188 (1992).
12. **Malby, R. L., Caldwell, J. B., Gruen, L. C., Harley, V. R., Ivancic, N., Kortt, A. A., Lilley, G. G., Power, B. E., Webster, R. G., Colman, P. M., and Hudson, P. J.:** Recombinant antineuraminidase single chain antibody: expression, characterization, and crystallization in complex with antigen, Proteins, **16**, 57–63 (1993).
13. **Tsumoto, K., Shinoki, K., Kondo, H., Uchikawa, M., Juji, T., and Kumagai, I.:** Highly efficient recovery of functional single-chain Fv fragments from inclusion bodies overexpressed in *Escherichia coli* by controlled introduction of oxidizing reagent–application to a human single-chain Fv fragment, J. Immunol. Methods, **219**, 119–129 (1998).
14. **Umetsu, M., Tsumoto, K., Hara, M., Ashish, K., Goda, S., Adschiri, T., and Kumagai, I.:** How additives influence the refolding of immunoglobulin-folded proteins in a stepwise dialysis system. Spectroscopic evidence for highly efficient refolding of a single-chain Fv fragment, J. Biol. Chem., **278**, 8979–8987 (2003).
15. **Asano, R., Sone, Y., Makabe, K., Tsumoto, K., Hayashi, H., Katayose, Y., Unno, M., Kudo, T., and Kumagai, I.:** Humanization of the bispecific epidermal growth factor receptor x CD3 diabody and its efficacy as a potential clinical reagent, Clin. Cancer Res., **12**, 4036–4042 (2006).
16. **Molineux, G.:** Pegylation: engineering improved biopharmaceuticals for oncology, Pharmacotherapy, **23**, 3S–8S (2003).
17. **Veronese, F. M. and Pasut, G.:** PEGylation, successful approach to drug delivery, Drug Discov. Today, **10**, 1451–1458 (2005).
18. **Hinds, K. D. and Kim, S. W.:** Effects of PEG conjugation on insulin properties, Adv. Drug Deliv. Rev., **54**, 505–530 (2002).
19. **George, A. J., Titus, J. A., Jost, C. R., Kurucz, I., Perez, P., Andrew, S. M., Nicholls, P. J., Huston, J. S., and Segal, D. M.:** Redirection of T cell-mediated cytotoxicity by a recombinant single-chain Fv molecule, J. Immunol., **152**, 1802–1811 (1994).
20. **Verma, R., Boleti, E., and George, A. J.:** Antibody engineering: comparison of bacterial, yeast, insect and mammalian expression systems, J. Immunol. Methods, **216**, 165–181 (1998).
21. **Laemmli, U. K.:** Cleavage of structural proteins during the assembly of the head of bacteriophage T4, Nature, **227**, 680–685 (1970).
22. **Asano, R., Watanabe, Y., Kawaguchi, H., Fukazawa, H., Nakanishi, T., Umetsu, M., Hayashi, H., Katayose, Y., Unno, M., Kudo, T., and Kumagai, I.:** Highly effective recombinant format of a humanized IgG-like bispecific antibody for cancer immunotherapy with retargeting of lymphocytes to tumor cells, J. Biol. Chem., **282**, 27659–27665 (2007).
23. **Huston, J. S., Levinson, D., Mudgett-Hunter, M., Tai, M. S., Novotny, J., Margolies, M. N., Ridge, R. J., Bruccoleri, R. E., Haber, E., Crea, R., and Oppermann, H.:** Protein engineering of antibody binding sites: recovery of specific activity in an anti-digoxin single-chain Fv analogue produced in *Escherichia coli*, Proc. Natl. Acad. Sci. U. S. A., **85**, 5879–5883 (1988).
24. **Gruber, M., Schodin, B. A., Wilson, E. R., and Kranz, D. M.:** Efficient tumor cell lysis mediated by a bispecific single chain antibody expressed in *Escherichia coli*, J. Immunol., **152**, 5368–5374 (1994).
25. **Holliger, P., Prospero, T., and Winter, G.:** "Diabodies": small bivalent and bispecific antibody fragments, Proc. Natl. Acad. Sci. U. S. A., **90**, 6444–6448 (1993).
26. **Kipriyanov, S. M., Moldenhauer, G., Schuhmacher, J., Cochlovius, B., Von der Lieth, C. W., Matys, E. R., and Little, M.:** Bispecific tandem diabody for tumor therapy with improved antigen binding and pharmacokinetics, J. Mol. Biol., **293**, 41–56 (1999).
27. **Hu, S., Shively, L., Raubitschek, A., Sherman, M., Williams, L. E., Wong, J. Y., Shively, J. E., and Wu, A. M.:** Minibody: a novel engineered anti-carcinoembryonic antigen antibody fragment (single-chain Fv-CH3) which exhibits rapid, high-level targeting of xenografts, Cancer Res., **56**, 3055–3061 (1996).
28. **Yang, K., Basu, A., Wang, M., Chintala, R., Hsieh, M. C., Liu, S., Hua, J., Zhang, Z., Zhou, J., and Li, M., et al.:** Tailoring structure-function and pharmacokinetic properties of single-chain Fv proteins by site-specific PEGylation, Protein Eng., **16**, 761–770 (2003).
29. **Ramm, K., Gehrig, P., and Pluckthun, A.:** Removal of the conserved disulfide bridges from the scFv fragment of an antibody: effects on folding kinetics and aggregation, J. Mol. Biol., **290**, 535–546 (1999).
30. **Buchner, J. and Rudolph, R.:** Renaturation, purification and characterization of recombinant Fab-fragments produced in *Escherichia coli*, Biotechnology. (N. Y)., **9**, 157–162 (1991).
31. **Qiao, Z. S., Guo, Z. Y., and Feng, Y. M.:** Putative disulfide-forming pathway of porcine insulin precursor during its refolding in vitro, Biochemistry, **40**, 2662–2668 (2001).
32. **Ahn, J. H., Lee, Y. P., and Rhee, J. S.:** Investigation of refolding condition for Pseudomonas fluorescens lipase by response surface methodology, J. Biotechnol., **54**, 151–160 (1997).
33. **Hayashi, H., Asano, R., Tsumoto, K., Katayose, Y., Suzuki, M., Unno, M., Kodama, H., Takemura, S., Yoshida, H., and Makabe, K., et al.:** A highly effective and stable bispecific diabody for cancer immunotherapy: cure of xenografted tumors by bispecific diabody and T-LAK cells, Cancer Immunol. Immunother., **53**, 497–509 (2004).

Please cite this article as: Kumagai, I., et al., Integration of PEGylation and refolding for renaturation of recombinant proteins from insoluble aggregates produced in bacteria–Application to a single-chain Fv fragment, J. Biosci. Bioeng. (2009), doi:10.1016/j.jbiosc.2009.10.016

the FEBS Journal

Application of the Fc fusion format to generate tag-free bi-specific diabodies

Ryutaro Asano[1], Keiko Ikoma[1], Hiroko Kawaguchi[1], Yuna Ishiyama[1], Takeshi Nakanishi[1], Mitsuo Umetsu[1], Hiroki Hayashi[2], Yu Katayose[2], Michiaki Unno[2], Toshio Kudo[3] and Izumi Kumagai[1]

1 Department of Biomolecular Engineering, Graduate School of Engineering, Tohoku University, Sendai, Japan
2 Division of Gastroenterological Surgery, Department of Surgery, Graduate School of Medicine, Tohoku University, Sendai, Japan
3 Cell Resource Center for Biomedical Research, Institute of Development, Aging and Cancer, Tohoku University, Sendai, Japan

Keywords
bi-specific diabody; Fc fusion format; preparation method; small therapeutic antibody; tag-free protein

Correspondence
I. Kumagai, Aoba 6-6-11-606, Aramaki, Aoba-ku, Sendai 980-8579, Japan
Fax: +81 22 795 6164
Tel: +81 22 795 7274
E-mail: kmiz@kuma.che.tohoku.ac.jp

(Received 1 May 2009, revised 9 November 2009, accepted 17 November 2009)

doi:10.1111/j.1742-4658.2009.07499.x

We previously reported the use of a humanized bi-specific diabody that targets epidermal growth factor receptor and CD3 (hEx3-Db) for cancer immunotherapy. Bacterial expression can be used to express small recombinant antibodies on a large scale; however, their overexpression often results in the formation of insoluble aggregates, and in most cases artificial affinity peptide tags need to be fused to the antibodies for purification by affinity chromatography. Here, we propose a novel method for preparing refined, functional, tag-free bi-specific diabodies from IgG-like bi-specific antibodies (BsAbs) in a mammalian expression system. We created an IgG-like BsAb in which bi-specific diabodies were fused to the human Fc region via a designed human rhinovirus 3C (HRV3C) protease recognition site. The BsAb was purified by protein A affinity chromatography, and the refined tag-free hEx3-Db was efficiently produced from the Fc fusion format by protease digestion. The tag-free hEx3-Db from the Fc fusion format showed a greater inhibition of cancer growth than affinity-tagged hEx3-Db prepared directly from Chinese hamster ovary cells. We also applied our novel method to another small recombinant antibody fragment, hEx3 single-chain diabody (hEx3-scDb), and demonstrated the versatility and advantages of our proposed method compared with papain digestion of hEx3-scDb. This approach may be used for industrial-scale production of functional tag-free small therapeutic antibodies.

Introduction

Bi-specific antibodies (BsAbs) are attractive formats for recombinant antibodies that can bind to two different epitopes on antigens. This bi-specificity can be used in cancer immunotherapy by cross-linking tumor cells to immune cells such as cytotoxic T cells, natural killer cells and macrophages. This linkage accelerates the destruction of the tumor cells by immune cells, so that the dose of therapeutic antibodies can be reduced from that required in the case of mono-specific antibodies [1,2].

Abbreviations
BsAbs, bi-specific antibodies; CHO, Chinese hamster ovary; Db, diabody; EGFR, epidermal growth factor receptor; hEx3-Db, humanized bi-specific diabody that targets epidermal growth factor receptor and CD3; hEx3-scDb, hEx3 single-chain diabody; HRV3C, human rhinovirus 3C; MTS, 3-(4,5-dimethylthiazole-2-yl)-5-(3-carboxymethoxyphenyl)-2-(4-sulfophenyl)-2*H*-tetrazolium inner salt; scDb, single-chain diabody; scFv, single chain Fv; T-LAK, lymphokine-activated killer cells with the T-cell phenotype; tanDb, tandem single-chain diabody; taFv, tandem scFv.

Conventionally, BsAbs are produced by chemical conjugation or somatic fusion of two hybridomas, forming a quadroma that can produce bi-specific IgG molecules [1,3]. Clinical studies of these BsAbs have been performed, and some impressive local anti-tumor responses have been reported; however, these trials have also been limited by the occurrence of human anti-mouse antibody and/or Fc-mediated side-effects such as the induction of a cytokine storm [4,5]. Furthermore, these methods cannot be utilized for large-scale production, and a quadroma cannot control the heterogeneity of the antibodies produced; for instance, ten possible variants of antibodies can be generated when two heavy and two light chains are randomly associated. Therefore, steady production of homogeneous BsAbs requires the use of a host-vector system.

Advances in antibody engineering techniques and host-vector expression systems have facilitated the generation of recombinant BsAbs with improved properties. A variety of recombinant BsAbs have been developed from two antibody fragments such as single-chain Fv fragments (scFv; 25 kDa) [6,7], and diabodies (Db; 55 kDa) [8] that recognize different antigens. The most common BsAb formats that have been produced from these fragments are tandem scFv (taFv) [9], tandem single-chain diabodies (tandem scDb, tanDb) [10] and mini-bodies (dimeric scDb–CH3 fusion protein) [11]. Compared with classic BsAbs prepared by chemical conjugation or production of a quadroma, small antibody molecules, such as diabodies, are of a suitable size for rapid tissue penetration, high target retention and rapid clearance [12,13]. Their smaller size also enables expression of BsAbs in bacteria, and as the structure is composed only of antibody variable regions, this eliminates the Fc-mediated side-effects of BsAbs. Although the rapid blood clearance and monovalency of bi-specific diabodies, scDbs and taFv (all approximately 55 kDa) may limit their therapeutic application, engineering the length and amino acid composition of the middle linker in scDb, for example, may enable them to assemble into multimers, such as tanDb (114 kDa), with higher molecular weight and bivalency for each target antigen [14,15].

Small bi-specific antibody fragments prepared in bacteria are often expressed as insoluble aggregates in the cytoplasmic or periplasmic space [10,16–18], and require fusion of artificial affinity peptide tags, such as a polyhistidine tag, hemagglutinin tag or FLAG tag, at the N- or C-terminus of the BsAbs to allow complete removal of the vast amount of host-derived proteins by affinity chromatography [16,19]. The requirement for such tags raises concerns about immunogenicity. We have previously reported significant anti-tumor activity *in vitro* and *in vivo* for a humanized bi-specific diabody targeting epidermal growth factor receptor (EGFR) and CD3 (hEx3-Db) [20]. However, even though the yield of hEx3-Db was over 10 $mg \cdot L^{-1}$ culture, it was also expressed as insoluble aggregates, and fusion of an affinity tag was necessary for purification before the re-folding process.

We have also reported the construction of a mammalian expression system for affinity-tagged bi-specific diabodies and their Fc fusion formats [21]. Here, we developed a novel method for the production of highly purified tag-free diabodies using the mammalian expression system. Diagrams of the various gene constructs are shown in Fig. 1. The tag-free hEx3-Db alone was expressed sufficiently to be purified by ion-exchange chromatography. Expression of the hEx3 diabodies fused to the human Fc region via a designed protease recognition site enabled high-efficiency purification by protein A affinity chromatography and increased the yield of tag-free hEx3-Db. We also used our method to produce tag-free small BsAbs to hEx3-scDb. For hEx3-scDb, use of the designed protease recognition site had advantages over papain digestion, which caused unwanted degradation. Both tag-free hEx3-Db and hEx3-scDb prepared by restriction protease digestion from the Fc fusion format showed a greater inhibition of cancer growth *in vitro* than previously produced affinity-tagged diabodies directly prepared from the supernatant of Chinese hamster ovary (CHO) transfectants [21]. Thus, this approach appears to improve both the yield and efficacy of the bi-specific antibody fragments.

Results

Preparation of tag-free bi-specific diabodies

Tag-free hEx3-Db was directly secreted from mammalian cells and purified by cation-exchange chromatography as described in Experimental procedures. Purified hEx3-Db was applied to a gel filtration column for further analysis and purification (Fig. 2A). The first small peak, second large peak and the shoulder of the major peak seen in the chromatograph were identified as the multimeric, dimeric and monomeric structures of tag-free hEx3-Db, respectively. Equivalent amounts of hOHh5L (humanized OKT3 VH - linker - humanized 528 VL) and h5HhOL (humanized 528 VH - linker - humanized OKT3 VL) were confirmed in the dimeric fraction by SDS–PAGE analysis (Fig. 2B). Thus, purified tag-free hEx3-Dbs were obtained without affinity chromatography at a final yield of approximately 1 $mg \cdot L^{-1}$ culture.

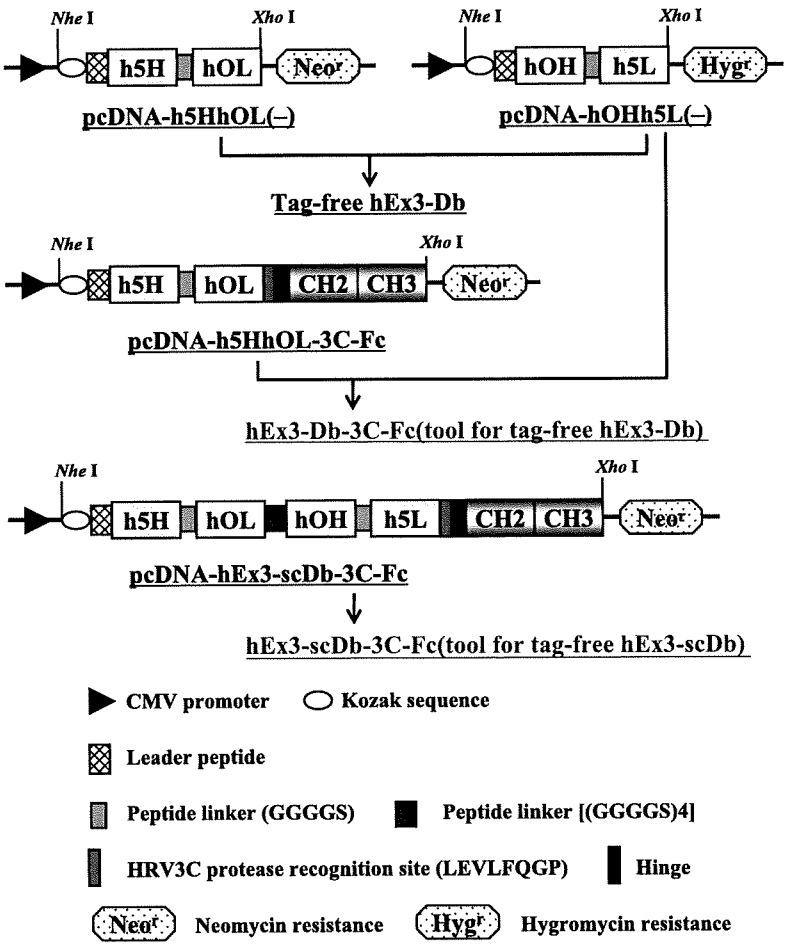

Fig. 1. Schematic illustration of the BsAb gene constructs in pCDNA3.1. The V^H and V^L regions of humanized 528 Fv are designated h5H and h5L, and those of humanized OKT3 Fv are designated hOH and hOL, respectively. The positions of important restriction enzyme sites used and the key components are shown.

To prepare the high-quality, tag-free bi-specific diabodies, we fused the hEx3-Db to the human IgG1 Fc region. We inserted a recognition site for HRV3C protease between the diabody fragments and the Fc portion of hEx3-Fc. A schematic illustration of the preparation of tag-free hEx3-Db from its Fc fusion format is shown in Fig. 3A. The expressed IgG-like BsAbs were purified by protein A affinity chromatography and digested using glutathione *S*-transferase (GST)-fused HRV3C protease. The treated solution was loaded onto a glutathione-immobilized column and then a protein A column to remove added protease and digested Fc. SDS–PAGE analysis of each purification step showed the successful preparation of tag-free hEx3-Db from its Fc fusion format (Fig. 3B). Gel filtration chromatography showed that tag-free hEx3-Db predominantly formed dimers, with a small amount of multimeric forms (Fig. 4A). The homogeneity of tag-free hEx3-Db in the eluted fraction was also confirmed by SDS–PAGE (Fig. 4B). The final yield of tag-free hEx3-Db from the Fc fusion format was approximately 5 $mg \cdot L^{-1}$ culture, i.e. five times that of the secreted tag-free hEx3-Db. Thus, secretion of BsAbs as the Fc fusion format increased the amount of prepared tag-free diabodies due to the high productivity (approximately 10 $mg \cdot L^{-1}$) and the efficient purification using protein A.

Mass spectrometry of tag-free bi-specific diabodies

We previously reported that the strong inter-domain interaction between cognate V^H and V^L domains of hEx3-Db leads to the spontaneous formation of functional heterodimers [22]. In the present study, the molecular weight of the monomorphous heterodimer of the tag-free hEx3-Db prepared from the Fc fusion format was confirmed by MALDI-TOF mass spectrometry (Fig. 4C). The mass spectrum for the diabodies prepared from the Fc fusion format had two peaks, one at *m/z* 26 424 and another at *m/z* 25 970, which correspond to the calculated molecular weights of

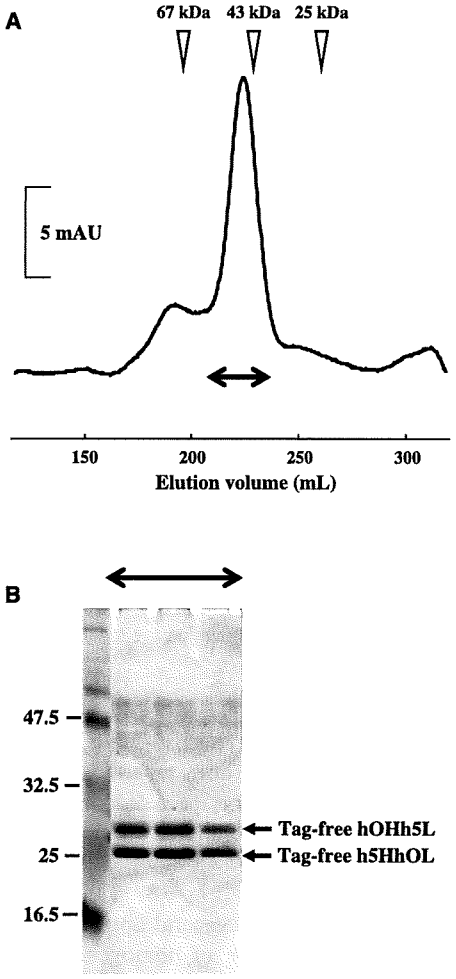

Fig. 2. (A) Gel filtration of tag-free hEx3-Db. The elution volume is shown on the *x* axis, and the molecular mass (kDa) is shown above. The eluted fractions containing the bi-specific diabody are indicated by the two-headed arrow. (B) SDS–PAGE analysis under reducing conditions of the eluted fraction. Molecular size markers are shown on the left.

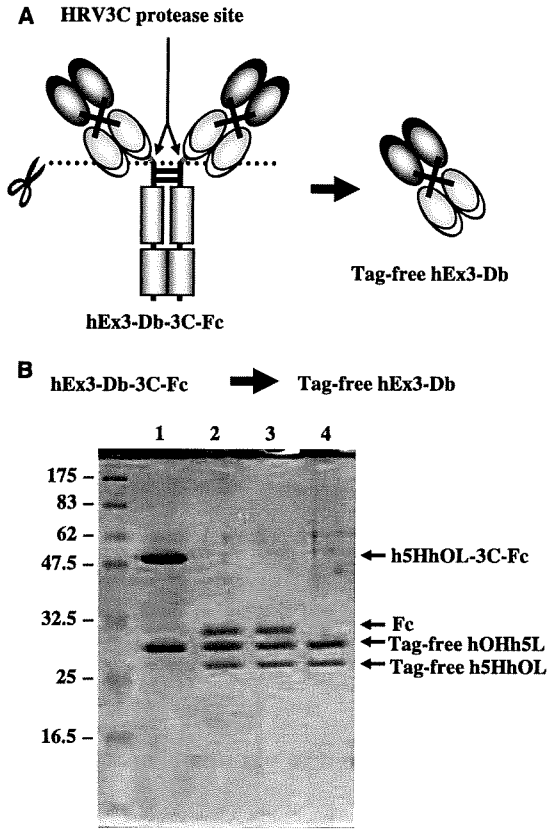

Fig. 3. (A) Schematic illustration of the hEx3-Db–3C–Fc fusion protein. The HRV3C protease cleavage site used for preparation of tag-free hEx3-Db is indicated. (B) Reducing SDS–PAGE of each purification step for preparation of tag-free hEx3-Db from hEx3-Db–3C–Fc. Lane 1, protein A chromatography-purified hEx3-Db–3C–Fc; lane 2, after HRV3C protease digestion; lane 3, after removal of HRV3C protease by glutathione Sepharose 4B chromatography; lane 4, purified tag-free hEx3-Db after removal of the Fc region by protein A chromatography.

hOHh5L digested from the Fc fusion (26 442) and h5HhOL without the peptide tag (25 991), respectively. These results indicate that Db–3C–Fc fusion proteins can serve as a tool for preparing tag-free diabodies with high yield and purity.

Binding affinity of tag-free bi-specific diabodies and its effect on growth inhibition

The binding affinity of tag-free hEx3-Dbs for CD3-positive lymphokine-activated killer cells with the T-cell phenotype (T-LAK cells) and EGFR-positive TFK-1 cells was measured by flow cytometry using polyclonal antibody to hEx3-Db. Tag-free hEx3-Dbs interacted with each targeted antigen (Fig. 5A), and the binding profiles were comparable with those previously reported for affinity-tagged hEx3-Db [20,22]. These results indicate that the diabody prepared by HRV3C protease digestion from the Fc fusion format retained sufficient binding activity and bi-specificity.

To evaluate the inhibition of cancer growth by tag-free hEx3-Db, an MTS assay was performed for TFK-1 cells by using T-LAK cells at an effector/target ratio of 5 : 1. Tag-free hEx3-Db prepared from the Fc fusion format inhibited cancer cell growth more effectively than did affinity-tagged hEx3-Db (Fig. 5B). Imperceptible differences in purity and local structural perturbations that are dependent on the preparation method might affect these activities.

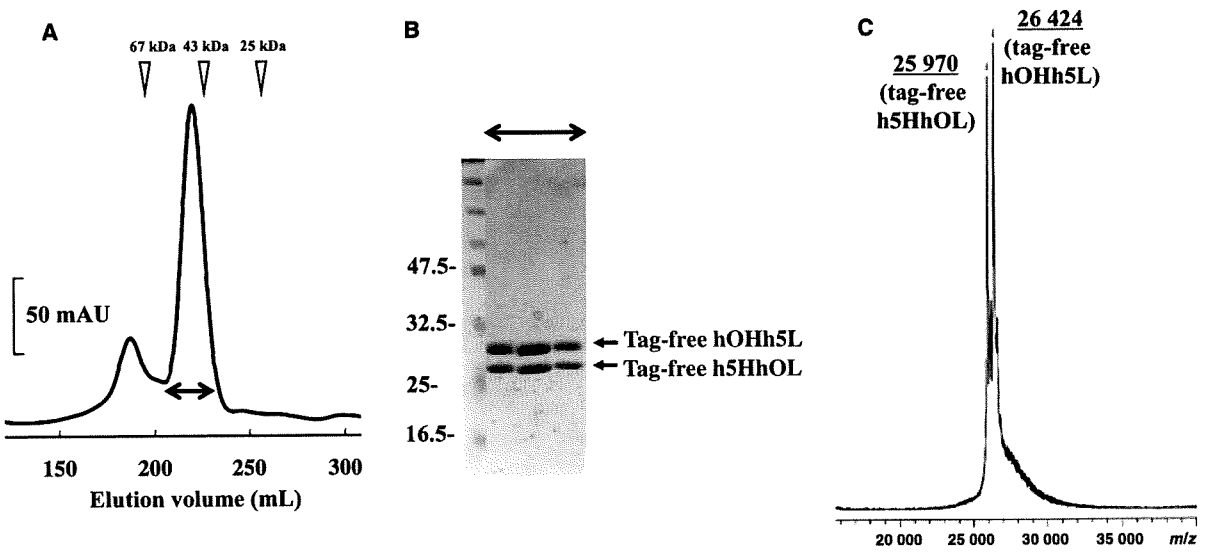

Fig. 4. (A) Gel filtration of purified hEx3-Db after removal of HRV3C protease and the Fc fragment. The elution volume is shown on the *x* axis, and the molecular mass (kDa) is shown above. The eluted fractions containing the bi-specific diabody are indicated by the two-headed arrow. (B) SDS–PAGE analysis under reducing conditions of the eluted fractions. Molecular size markers are shown on the left. (C) MALDI-TOF mass spectra of the tag-free hEx3-Db prepared from hEx3-Db–3C–Fc.

Application of method to tag-free bi-specific single-chain diabody

To demonstrate the utility of this novel method, we applied it to the preparation of tag-free hEx3-scDb, which is a single-chain form of hEx3-Db (Fig 6A). An HRV3C protease recognition site was inserted between hEx3-scDb and the Fc portion, and the recognition sequence for papain was conserved. Papain is a cysteine protease that is generally used in the preparation of Fab fragments from IgG, because the recognition site for papain naturally exists around the hinge region of intact antibody.

When we digested hEx3-scDb–3C–Fc with HRV3C protease, hEx3-scDb was separated from the Fc portion with no degradation. Similar to the tag-free hEx3-Db, the Fc portion was completely removed by protein A affinity chromatography (Fig. 6B). To confirm the benefit of the design of the HRV3C protease digestion site, we also followed the time course of papain digestion of hEx3-scDb–3C–Fc (Fig. 6C). Although tag-free hEx3-scDb was successfully prepared by papain digestion, especially with an incubation time of 1 h, two unexpected bands corresponding to hOHh5L and h5HhOL caused by a break in the middle linker from scDb also appeared. This digestion proceeded as the incubation time increased, and further degradation of h5HhOL was observed after incubation for 10 h.

The binding affinity of tag-free hEx3-scDb prepared from the Fc fusion format for both targeted cells was confirmed by flow cytometry (Fig. 7A), and its enhanced cytotoxicity was compared with affinity-tagged hEx3-scDb [21] in the MTS assay with the use of T-LAK cells as effector cells (Fig. 7B). These results strongly support the utility and general applicability of our method for the preparation of homogeneous tag-free small recombinant antibodies.

Discussion

Recombinant BsAbs have several advantages over classic BsAbs prepared by chemical cross-linkage or fusion of two hybridoma clones [16,23–25]. The IgG-like BsAbs containing human Fc regions are highly effective recombinant antibodies [25–27] because of the antibody-dependent cellular cytotoxicity effect. By comparison, small bi-specific diabodies without Fc have the advantages of rapid tissue penetration, high target retention and a distance between the two antigen-binding sites of the diabodies that is large enough to bring two cells together for recruitment of immune cells [1,2,28].

Large-scale production of bi-specific diabodies in bacterial expression systems would be expected because of their small size; however, the yield is typically only a few mg per L in most cases [10,16,17]. We previously proposed an *in vitro* refolding system to prepare

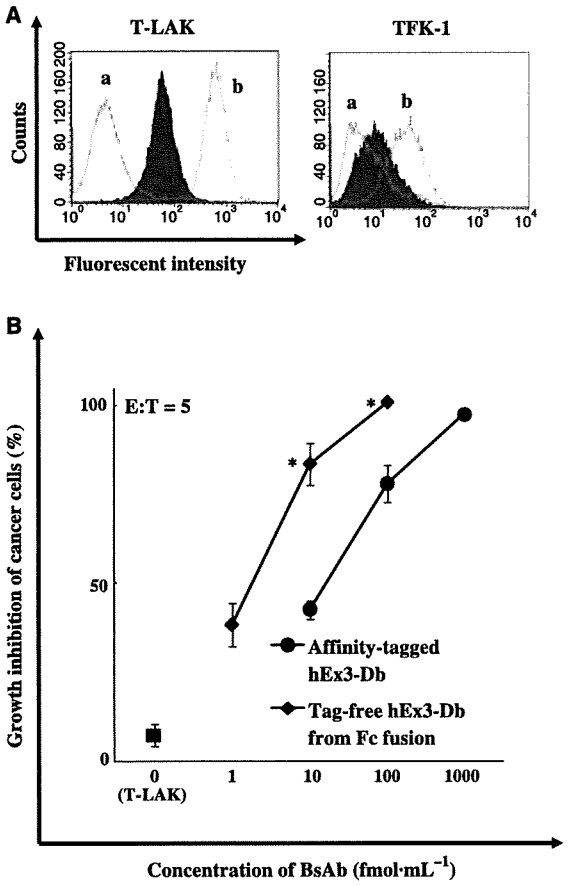

Fig. 5. (A) Flow cytometry analysis of tag-free hEx3-Db prepared from hEx3-Db–3C–Fc. Cells were incubated with NaCl/P_i as a negative control (a) and with either OKT3 parental IgG (for T-LAK cells) or 528 IgG (for TFK-1 cells), followed by staining with fluorescein isothiocyanate-conjugated anti-mouse IgG as a positive control (b). The shaded areas correspond to the fluorescence intensity distributions of the cells incubated with hEx3-Db. Each mixture was stained with rabbit anti-hEx3-Db serum followed by fluorescein isothiocyanate-conjugated anti-rabbit IgG. (B) Growth inhibition of EGFR-positive TFK-1 cells by tag-free and affinity-tagged hEx3 diabodies. Each bi-specific diabody and T-LAK cells (effectors, E) were added to TFK-1 cells (T) at a ratio of 5 : 1. The tag-free hEx3-Db inhibited growth significantly better (*$P < 0.005$) than the affinity-tagged hEx3-Db did [21]. Data are mean values ± SD and are representative of at least three independent experiments with similar results.

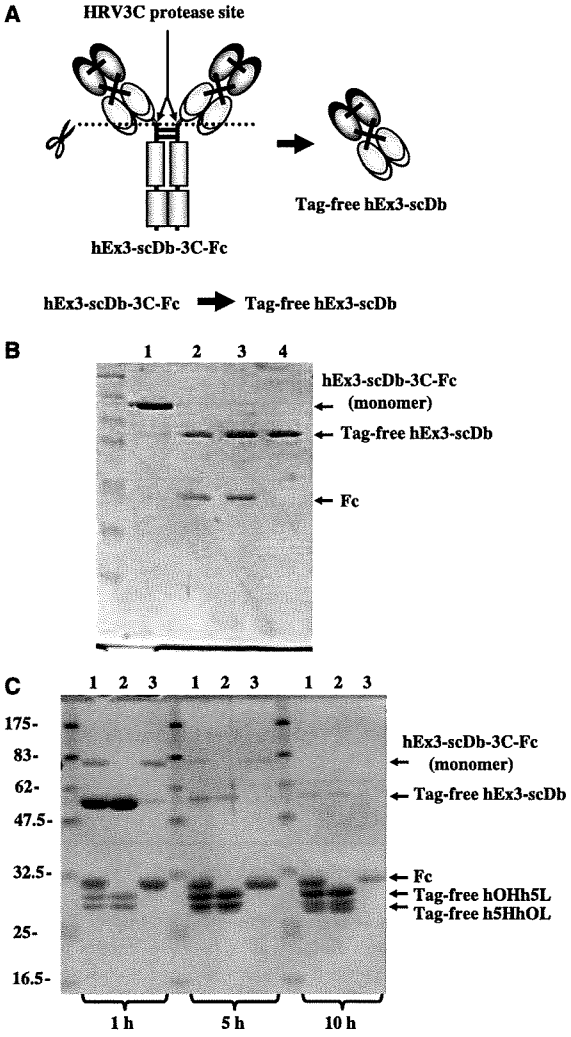

Fig. 6. (A) Schematic illustration of the hEx3-scDb–3C–Fc fusion protein. The HRV3C protease cleavage site used for preparation of tag-free hEx3-scDb is indicated. (B) Reducing SDS–PAGE of each purification step for preparation of tag-free hEx3-scDb from hEx3-scDb–3C–Fc. Lane 1, protein A chromatography-purified hEx3-scDb–3C–Fc; lane 2, after HRV3C protease digestion; lane 3, after removal of HRV3C protease by glutathione Sepharose 4B chromatography; lane 4, purified tag-free hEx3-scDb after removal of the Fc region by protein A chromatography. (C) Reducing SDS–PAGE of hEx3-scDb–3C–Fc incubated with papain for 1, 5 and 10 h. Lane 1, digested hEx3-scDb–3C–Fc; lane 2, flowthrough from protein A chromatography; lane 3, eluted protein from protein A chromatography.

functional bi-specific diabodies from the insoluble fraction, but solubilizing the expressed proteins from insoluble fraction required purification from the vast amount of host-derived proteins, which forced us to utilize an artificial tag [20,22,29]. The immunogenicity of the artificial peptide tag has not been determined, and preparation of tag-free formats from insoluble fractions may be difficult to achieve [16]. For these reasons, a new preparation method for bi-specific diabodies was needed that required minimal artificial amino acid sequences and produced high yields.

In the present study, we successfully purified tag-free hEx3-Db from the supernatant of transfected CHO

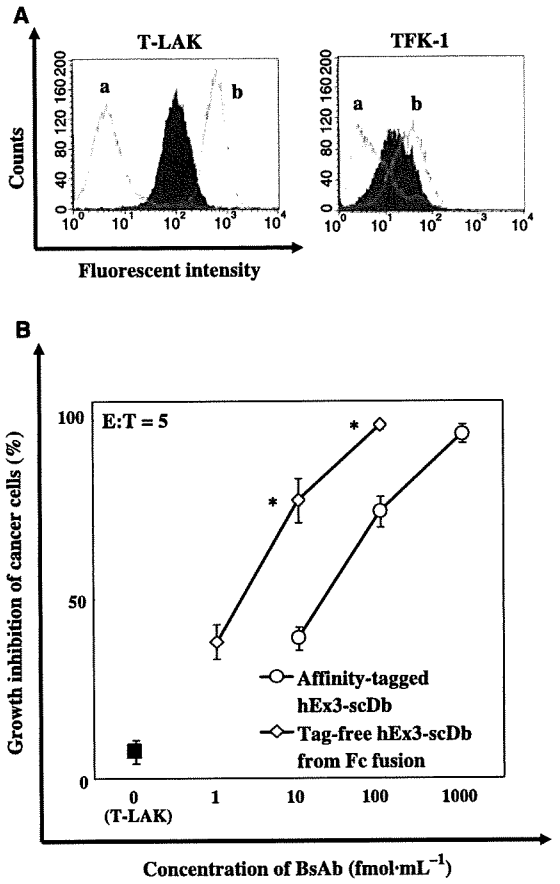

Fig. 7. (A) Flow cytometric analysis of purified tag-free hEx3-scDb. Cells were incubated with NaCl/P_i as a negative control (a) and with either OKT3 parental IgG (for T-LAK cells) or 528 IgG (for TFK-1 cells), followed by staining with fluorescein isothiocyanate-conjugated anti-mouse IgG as a positive control (b). The shaded areas correspond to the fluorescence intensity distributions of the cells incubated with hEx3-Db. Each mixture was stained with rabbit anti-hEx3-Db serum followed by fluorescein isothiocyanate-conjugated anti-rabbit IgG. (B) Growth inhibition of EGFR-positive TFK-1 cells by tag-free and affinity-tagged hEx3 single-chain diabodies. Each bi-specific diabody and T-LAK cells (effectors, E) were added to TFK-1 cells (T) at a ratio of 5 : 1. The tag-free hEx3-scDb inhibited growth significantly better (*$P < 0.005$) than the affinity-tagged hEx3-scDb did [21]. Data are mean values ± SD and are representative of at least three independent experiments with similar results.

cells using cation-exchange and gel filtration chromatography (Fig. 2). However, the final yield of this secreted tag-free hEx3-Db was approximately 1 mg·L^{-1} culture. We thus developed a novel method using IgG-like BsAb and a restriction protease with high specificity. The fusion of Fc to diabodies resulted in high productivity and enabled affinity purification using protein A. The homogeneous dimer structure and molecular weight of the tag-free hEx3-Db prepared from the Fc fusion format (hEx3-Db–3C–Fc) were confirmed by gel filtration and mass spectrometry, and the yield was approximately five times that of the directly secreted tag-free hEx3-Db (Figs 3 and 4).

The specific binding affinity and bi-specificity of the tag-free hEx3-Db for T-LAK and TFK-1 cells were observed by flow cytometry (Fig. 5A). Interestingly, the result of the MTS assay showed that growth inhibition by tag-free hEx3-Db from the Fc fusion was more intense than that by affinity-tagged hEx3-Db (Fig. 5B). Although it is unclear why the tag-free diabodies prepared from the Fc fusion format had such high activity, imperceptible differences in purity and local structural perturbations that are dependent on the preparation method might have affected the activity of the diabodies. The reasons for this difference in activity are now under investigation. Furthermore, we were able to reproduce our results with tag-free hEx3-scDb, which indicates the utility and applicability of our method for the preparation of tag-free small recombinant antibodies (Figs 6 and 7). The single-chain format has additional advantages: scDbs can be produced from a single expression vector and are expected to have improved stability *in vivo* because the two chains in the diabody are connected to each other via a linker [14,30].

In general, papain and pepsin have been used in the preparation of antibody fragments from IgG-like antibodies, and successful preparation of scFv from scFv–Fc has also been reported [31]. However, for hEx3 single-chain diabodies fused with Fc, papain digestion led to undesired degradation (Fig. 6C). Thus, the advantages of using the designed protease recognition site were confirmed, especially in recombinant antibodies that included a number of artificial sequences.

To date, several different small BsAb formats have been proposed to increase efficacy and availability, such as scDbs [30], taFv [9,32] and mini-bodies [11]. Further, dimeric scDbs known as tanDbs, with bivalency for each target antigen, can be produced by engineering the length and amino acid composition of middle linker of scDb [15]. Here, we selected diabodies and scDb monomers with a 20-amino-acid middle linker [$(GGGGS)_4$] as small BsAbs, because they are one of the simplest construction formats [20,22]. Use of our preparation method for other BsAbs formats is currently in progress.

We previously reported for BsAbs with affinity peptide tags that hEx3-scDb has comparable function to that of hEx3-Db *in vitro* [22]. In this work, we have shown that tag-free formats behave quantitatively

similarly in *in vitro* cell growth inhibition studies (Figs 5B and 7B). Therefore, regardless of the presence or absence of an affinity tag, the activity of hEx3-Db is comparable to that of hEx3-scDb. Several reports have demonstrated a higher stability of scDb than other formats such as Db and taFv [14,33–35]. Although hEx3-Db and hEx3-scDb showed similar activities *in vitro*, there is a possibility the hEx3-scDb may exhibit a higher activity *in vivo* because of higher stability. Stability tests under physiological conditions between hEx3-Db and hEx3-scDb are currently in progress.

Issues such as rapid blood clearance and the relatively low affinity caused by low molecular weight and monovalent binding may limit the therapeutic application of bi-specific diabodies [14]. In such cases, conversion into more effective formats such as tanDb may be required. The approach described here is also expected to be applicable for convenient preparation of such antibody fragments.

In conclusion, we prepared tag-free bi-specific diabodies in a mammalian expression system and developed a novel method using IgG-like antibodies and protease digestion to prepare highly purified, tag-free bi-specific diabodies. Our method may allow industrial-scale production of functional tag-free small biological agents such as small recombinant antibodies.

Experimental procedures

Preparation of secreted Ex3 diabodies

In accordance with the convention used in a previous report, we describe the two hetero scFvs of hEx3-Db as h5HhOL and hOHh5L [20]. The gene constructs (Fig. 1) were inserted into pcDNA3.1/Neo or pcDNA3.1/Hygro mammalian expression vectors (both from Invitrogen, Groningen, Netherlands). The leader peptide sequences for protein secretion were derived from the mouse OKT3 IgG [36]. The methods for expression and purification of the affinity-tagged hEx3-Db and hEx3-scDb have been described previously [21]. For production of tag-free hEx3-Db, CHO cells were co-transfected with pcDNA-h5HhOL (–) and pcDNA-hOHh5L(–) (Fig. 1), and cell clones expressing tag-free hEx3-Db were established in the presence of neomycin (G418) and hygromycin as described previously [21]. CHO clones that stably expressed tag-free hEx3-Db were selected by screening for a growth inhibition effect of each individual clone. The established CHO clone was cultured as previously described [27]. The secreted tag-free hEx3-Db was purified from pooled supernatants using a 5 mL HiTrap SP XL column (GE Healthcare Bio-Science Corp., Piscataway, NJ, USA) with a 5–250 mM gradient of NaCl in 50 mM phosphate solution (pH 6.0).

Preparation of tag-free hEx3 diabodies from the Fc fusion format

To construct the expression vector for preparing tag-free diabodies by using IgG-like BsAbs, we connected the hEx3 diabodies and the human IgG1 Fc region via a recognition site (LEVLFQGP) for human rhinovirus 3C (HRV3C) protease. CHO cells were co-transfected with equal amounts of the pcDNA-h5HhOL-3C-Fc and pcDNA-hOHh5L(–) vectors (Fig. 1), and grown in presence of neomycin (G418) and hygromycin as described previously [21]. A CHO clone that stably expressed the hEx3-Db–3C–Fc fusion protein was selected in a manner similar to that for tag-free hEx3-Db. For tag-free hEx3-scDb, CHO cells were transfected with the pcDNA-hEx3-scDb–3C–Fc vector, and selection for a stably expressed clone was performed in the presence of 500 $\mu g \cdot mL^{-1}$ of G418 (Nacalai Tesque, Kyoto, Japan).

IgG-like BsAbs of hEx3–3C–Fc and hEx3-scDb–3C–Fc were first purified by affinity chromatography on a protein A column (GE Healthcare) and then digested by HRV3C protease fused to GST (PreScission protease; GE Healthcare) according to the protocol described by the manufacturer. The protease was removed using a glutathione Sepharose 4B column (GE Healthcare), and the flow-through was re-loaded onto the protein A column to remove the digested Fc and undigested hEx3-scDb–3C–Fc fusion protein. The presence of the BsAbs in each stage of purification were confirmed by SDS–PAGE under reducing conditions.

To illustrate the applicability of this novel method, papain digestion of hEx3-scDb–3C–Fc was performed by use of an ImmunoPure Fab preparation kit (Thermo Fisher Scientific Inc., Rockford, IL, USA). The influence of papain digestion was confirmed by SDS–PAGE analysis under reducing conditions at 1, 5 and 10 h after digestion.

Gel filtration chromatography

Gel filtration analysis with a Hiload Superdex 200 pg column (26/60; GE Healthcare) was used to evaluate the structure of the bi-specific diabodies. The column was equilibrated using NaCl/P_i, and then 5 mL of purified recombinant antibodies was applied to the column at a flow rate of 2.5 $mL \cdot min^{-1}$.

Mass spectrometry

Mass spectra were measured using a REFLEX III MALDI-TOF mass spectrometer (Bruker Daltonics Inc., Billerica, MA, USA) equipped with a nitrogen laser (337 nm). Sinapic acid was applied as a matrix, and was dissolved to saturation in water:acetonitrile (2 : 1 v/v) containing 0.067% trifluoroacetic acid. Sample solutions from each stage were mixed with the sinapic acid-saturated solution in a 1 : 1 v/v ratio, and then 1 μL of the mixed

solution was loaded onto the sample target. After co-crystallization on the target, the crystals were washed twice with 2 μL of water containing 0.1% trifluoroacetic acid to remove residual salts. Analysis was performed in positive and linear modes with an accelerating voltage of 27 kV, and 200 scans were averaged. The spectra obtained were calibrated externally using the $[M + H^+]$ ions from two protein standards: cytochrome *c* from horse heart (*m/z* 12 360.08) and bovine trypsin (*m/z* 23 311.53) [37].

Preparation of T-LAK cells

Peripheral blood mononuclear cells were isolated by density-gradient centrifugation of heparin-containing blood from healthy volunteers. To induce proliferation of T-LAK cells, peripheral blood mononuclear cells were cultured for 48 h at a density of 1×10^6 cells per mL in medium supplemented with 100 $IU \cdot mL^{-1}$ of recombinant human IL-2 (kindly supplied by Shionogi Pharmaceutical Co., Osaka, Japan) in a culture flask (A/S Nunc, Roskilde, Denmark) that had been pre-coated with OKT3 monoclonal antibody (10 $\mu g \cdot mL^{-1}$). Proliferated cells were then transferred to another flask, and expanded for 2–3 weeks in a culture medium containing 100 $IU \cdot mL^{-1}$ IL-2, as reported previously [38].

Flow cytometric analyses

Test cells (1×10^6) were incubated on ice with 200 pmol of BsAb for 30 min. After washing with $NaCl/P_i$ containing 0.1% NaN_3, they were exposed for 30 min on ice to rabbit anti-hEx3-Db serum (kindly supplied by Immuno-Biological Laboratories Co. Ltd, Gunma, Japan) as the second antibody, and fluorescein isothiocyanate-conjugated anti-rabbit IgG (Santa Cruz Biotechnology, Santa Cruz, CA, USA) as the third antibody. The stained cells were analyzed by flow cytometry (FACSCalibur, Becton Dickinson, San Jose, CA, USA) [20].

In vitro growth inhibition assay

In vitro growth inhibition of TFK-1 (human bile duct carcinoma) was assayed using a 3-(4,5-dimethylthiazole-2-yl)-5-(3-carboxymethoxyphenyl)-2-(4-sulfophenyl)-2*H*-tetrazolium inner salt (MTS) assay kit (CellTiter 96 aqueous non-radioactive cell proliferation assay; Promega, Madison, WI, USA) as reported previously [39].

Acknowledgements

This work was supported by Grants-in-Aid for Scientific Research from the Ministry of Education, Science, Sports, and Culture of Japan (to R.A. and I.K.) and by grants from the New Energy and Industrial Technology Development Organization of Japan. Additional support was provided through the Program for Promotion of Fundamental Studies in Health Sciences of the National Institute of Biomedical Innovation.

References

1 Cao Y & Lam L (2003) Bispecific antibody conjugates in therapeutics. *Adv Drug Deliv Rev* **55**, 171–197.
2 Kufer P, Lutterbuse R & Baeuerle PA (2004) A revival of bispecific antibodies. *Trends Biotechnol* **22**, 238–244.
3 Koelemij R, Kuppen PJ, van de Velde CJ, Fleuren GJ, Hagenaars M & Eggermont AM (1999) Bispecific antibodies in cancer therapy, from the laboratory to the clinic. *J Immunother* **22**, 514–524.
4 Segal DM, Weiner GJ & Weiner LM (1999) Bispecific antibodies in cancer therapy. *Curr Opin Immunol* **11**, 558–562.
5 van Spriel AB, van Ojik HH & van De Winkel JG (2000) Immunotherapeutic perspective for bispecific antibodies. *Immunol Today* **21**, 391–397.
6 Bird RE, Hardman KD, Jacobson JW, Johnson S, Kaufman BM, Lee SM, Lee T, Pope SH, Riordan GS & Whitlow M (1988) Single-chain antigen-binding proteins. *Science* **242**, 423–426.
7 Huston JS, Levinson D, Mudgett-Hunter M, Tai MS, Novotny J, Margolies MN, Ridge RJ, Bruccoleri RE, Haber E, Crea R *et al.* (1988) Protein engineering of antibody binding sites: recovery of specific activity in an anti-digoxin single-chain Fv analogue produced in *Escherichia coli*. *Proc Natl Acad Sci USA* **85**, 5879–5883.
8 Holliger P, Prospero T & Winter G (1993) 'Diabodies': small bivalent and bispecific antibody fragments. *Proc Natl Acad Sci USA* **90**, 6444–6448.
9 Schlereth B, Fichtner I, Lorenczewski G, Kleindienst P, Brischwein K, da Silva A, Kufer P, Lutterbuese R, Junghahn I, Kasimir-Bauer S *et al.* (2005) Eradication of tumors from a human colon cancer cell line and from ovarian cancer metastases in immunodeficient mice by a single-chain Ep-CAM-/CD3-bispecific antibody construct. *Cancer Res* **65**, 2882–2889.
10 Arndt MA, Krauss J, Kipriyanov SM, Pfreundschuh M & Little M (1999) A bispecific diabody that mediates natural killer cell cytotoxicity against xenotransplantated human Hodgkin's tumors. *Blood* **94**, 2562–2568.
11 Shahied LS, Tang Y, Alpaugh RK, Somer R, Greenspon D & Weiner LM (2004) Bispecific minibodies targeting HER2/neu and CD16 exhibit improved tumor lysis when placed in a divalent tumor antigen binding format. *J Biol Chem* **279**, 53907–53914.
12 Robinson MK, Doss M, Shaller C, Narayanan D, Marks JD, Adler LP, Gonzalez Trotter DE & Adams GP (2005) Quantitative immuno-positron emission

tomography imaging of HER2-positive tumor xenografts with an iodine-124 labeled anti-HER2 diabody. *Cancer Res* **65**, 1471–1478.
13 Sundaresan G, Yazaki PJ, Shively JE, Finn RD, Larson SM, Raubitschek AA, Williams LE, Chatziioannou AF, Gambhir SS & Wu AM (2003) ^{124}I-labeled engineered anti-CEA minibodies and diabodies allow high-contrast, antigen-specific small-animal PET imaging of xenografts in athymic mice. *J Nucl Med* **44**, 1962–1969.
14 Kipriyanov SM, Moldenhauer G, Schuhmacher J, Cochlovius B, Von der Lieth CW, Matys ER & Little M (1999) Bispecific tandem diabody for tumor therapy with improved antigen binding and pharmacokinetics. *J Mol Biol* **293**, 41–56.
15 Le Gall F, Reusch U, Little M & Kipriyanov SM (2004) Effect of linker sequences between the antibody variable domains on the formation, stability and biological activity of a bispecific tandem diabody. *Protein Eng Des Sel* **17**, 357–366.
16 Peipp M & Valerius T (2002) Bispecific antibodies targeting cancer cells. *Biochem Soc Trans* **30**, 507–511.
17 Helfrich W, Kroesen BJ, Roovers RC, Westers L, Molema G, Hoogenboom HR & de Leij L (1998) Construction and characterization of a bispecific diabody for retargeting T cells to human carcinomas. *Int J Cancer* **76**, 232–239.
18 Tsumoto K, Shinoki K, Kondo H, Uchikawa M, Juji T & Kumagai I (1998) Highly efficient recovery of functional single-chain Fv fragments from inclusion bodies overexpressed in *Escherichia coli* by controlled introduction of oxidizing reagent – application to a human single-chain Fv fragment. *J Immunol Methods* **219**, 119–129.
19 Skerra A & Schmidt TG (2000) Use of the Strep-Tag and streptavidin for detection and purification of recombinant proteins. *Methods Enzymol* **326**, 271–304.
20 Asano R, Sone Y, Makabe K, Tsumoto K, Hayashi H, Katayose Y, Unno M, Kudo T & Kumagai I (2006) Humanization of the bispecific epidermal growth factor receptor x CD3 diabody and its efficacy as a potential clinical reagent. *Clin Cancer Res* **12**, 4036–4042.
21 Asano R, Kawaguchi H, Watanabe Y, Nakanishi T, Umetsu M, Hayashi H, Katayose Y, Unno M, Kudo T & Kumagai I (2008) Diabody-based recombinant formats of humanized IgG-like bispecific antibody with effective retargeting of lymphocytes to tumor cells. *J Immunother* **31**, 752–761.
22 Asano R, Sone Y, Ikoma K, Hayashi H, Nakanishi T, Umetsu M, Katayose Y, Unno M, Kudo T & Kumagai I (2008) Preferential heterodimerization of a bispecific diabody based on a humanized anti-EGFR antibody 528. *Protein Eng Des Sel* **21**, 597–603.
23 Presta L (2003) Antibody engineering for therapeutics. *Curr Opin Struct Biol* **13**, 519–525.
24 Kontermann RE (2005) Recombinant bispecific antibodies for cancer therapy. *Acta Pharmacol Sin* **26**, 1–9.
25 Marvin JS & Zhu Z (2005) Recombinant approaches to IgG-like bispecific antibodies. *Acta Pharmacol Sin* **26**, 649–658.
26 Carter P (2001) Bispecific human IgG by design. *J Immunol Methods* **248**, 7–15.
27 Asano R, Watanabe Y, Kawaguchi H, Fukazawa H, Nakanishi T, Umetsu M, Hayashi H, Katayose Y, Unno M, Kudo T *et al.* (2007) Highly effective recombinant format of a humanized IgG-like bispecific antibody for cancer immunotherapy with retargeting of lymphocytes to tumor cells. *J Biol Chem* **282**, 27659–27665.
28 Perisic O, Webb PA, Holliger P, Winter G & Williams RL (1994) Crystal structure of a diabody, a bivalent antibody fragment. *Structure* **2**, 1217–1226.
29 Asano R, Kudo T, Nishimura Y, Makabe K, Hayashi H, Suzuki M, Tsumoto K & Kumagai I (2002) Efficient construction of a diabody using a refolding system: anti-carcinoembryonic antigen recombinant antibody fragment. *J Biochem* **132**, 903–909.
30 Alt M, Muller R & Kontermann RE (1999) Novel tetravalent and bispecific IgG-like antibody molecules combining single-chain diabodies with the immunoglobulin gamma1 Fc or CH3 region. *FEBS Lett* **454**, 90–94.
31 Wu AM, Tan GJ, Sherman MA, Clarke P, Olafsen T, Forman SJ & Raubitschek AA (2001) Multimerization of a chimeric anti-CD20 single-chain Fv–Fc fusion protein is mediated through variable domain exchange. *Protein Eng* **14**, 1025–1033.
32 Goel A, Beresford GW, Colcher D, Pavlinkova G, Booth BJ, Baranowska-Kortylewicz J & Batra SK (2000) Divalent forms of CC49 single-chain antibody constructs in *Pichia pastoris*: expression, purification, and characterization. *J Biochem* **127**, 829–836.
33 Brusselbach S, Korn T, Volkel T, Muller R & Kontermann RE (1999) Enzyme recruitment and tumor cell killing *in vitro* by a secreted bispecific single-chain diabody. *Tumor Target* **4**, 115–123.
34 Kipriyanov SM, Moldenhauer G, Braunagel M, Reusch U, Cochlovius B, Le Gall F, Kouprianova OA, Von der Lieth CW & Little M (2003) Effect of domain order on the activity of bacterially produced bispecific single-chain Fv antibodies. *J Mol Biol* **330**, 99–111.
35 Korn T, Nettelbeck DM, Volkel T, Muller R & Kontermann RE (2004) Recombinant bispecific antibodies for the targeting of adenoviruses to CEA-expressing tumour cells: a comparative analysis of bacterially expressed single-chain diabody and tandem scFv. *J Gene Med* **6**, 642–651.
36 Arakawa F, Kuroki M, Kuwahara M, Senba T, Ozaki H, Matsuoka Y, Misumi Y, Kanda H & Watanabe T (1996) Cloning and sequencing of the V^H and V^K genes of an anti-CD3 monoclonal antibody, and construction

of a mouse/human chimeric antibody. *J Biochem* **120**, 657–662.

37 Umetsu M, Tsumoto K, Hara M, Ashish K, Goda S, Adschiri T & Kumagai I (2003) How additives influence the refolding of immunoglobulin-folded proteins in a stepwise dialysis system. Spectroscopic evidence for highly efficient refolding of a single-chain Fv fragment. *J Biol Chem* **278**, 8979–8987.

38 Hayashi H, Asano R, Tsumoto K, Katayose Y, Suzuki M, Unno M, Kodama H, Takemura S, Yoshida H, Makabe K *et al.* (2004) A highly effective and stable bispecific diabody for cancer immunotherapy: cure of xenografted tumors by bispecific diabody and T-LAK cells. *Cancer Immunol Immunother* **53**, 497–509.

39 Asano R, Kudo T, Makabe K, Tsumoto K & Kumagai I (2002) Antitumor activity of interleukin-21 prepared by novel refolding procedure from inclusion bodies expressed in *Escherichia coli*. *FEBS Lett* **528**, 70–76.

Supplemental Material can be found at:
http://www.mcponline.org/cgi/content/full/M900179-MCP200/DC2

An Integrated Approach of Differential Mass Spectrometry and Gene Ontology Analysis Identified Novel Proteins Regulating Neuronal Differentiation and Survival*[S]

Daiki Kobayashi‡, Jiro Kumagai§, Takashi Morikawa‡, Masayo Wilson-Morifuji‡, Anthony Wilson‡, Atsushi Irie¶, and Norie Araki‡‖

MS-based quantitative proteomics is widely used for large scale identification of proteins. However, an integrated approach that offers comprehensive proteome coverage, a tool for the quick categorization of the identified proteins, and a standardized biological study method is needed for helping the researcher focus on investigating the proteins with biologically important functions. In this study, we utilized isobaric tagging for relative and absolute quantification (iTRAQ)-based quantitative differential LC/MS/MS, functional annotation with a proprietary gene ontology tool (Molecular Annotation by Gene Ontology (MANGO)), and standard biochemical methods to identify proteins related to neuronal differentiation in nerve growth factor-treated rat pheochromocytoma (PC12) cells, which serve as a representative model system for studying neuronal biological processes. We performed MS analysis by using both nano-LC-MALDI-MS/MS and nano-LC-ESI-MS/MS for maximal proteome coverage. Of 1,482 non-redundant proteins semiquantitatively identified, 72 were differentially expressed with 39 up- and 33 down-regulated, including 64 novel nerve growth factor-responsive PC12 proteins. Gene ontology analysis of the differentially expressed proteins by MANGO indicated with statistical significance that the up-regulated proteins were mostly related to the biological processes of cell morphogenesis, apoptosis/survival, and cell differentiation. Some of the up-regulated proteins of unknown function, such as PAIRBP1, translationally controlled tumor protein, prothymosin α, and MAGED1, were further analyzed to validate their significant functions in neuronal differentiation by immunoblotting and immunocytochemistry using each antibody combined with a specific short interfering RNA technique. Knockdown of these proteins caused abnormal cell morphological changes, inhibition of neurite formation, and cell death during each course of the differentiation, confirming their important roles in neurite formation and survival of PC12 cells. These results show that our iTRAQ-MANGO-biological analysis framework, which integrates a number of standard proteomics strategies, is effective for targeting and elucidating the functions of proteins involved in the cellular biological process being studied. ***Molecular & Cellular Proteomics 8:2350–2367, 2009.***

MS-based quantitative proteomics strategies such as iTRAQ[1] (1) and stable isotope labeling with amino acids in cell culture (2) are powerfully effective for the comprehensive characterization of biological phenomena (1–5). Although these methods have been applied for cancer biomarker (6, 7) and drug target (8) discovery, their use in the elucidation of biological and functional processes has been limited because of certain technical problems that arise when attempting to meaningfully process the immense amount of data obtained from such experiments. The following four main issues are typically the sources of such difficulties. 1) Quantitative identification by one type of MS system may fail to cover the total proteome because of ionization efficiency differences, such as those between ESI and MALDI, for certain peptides, leading to theoretical limitations in proteome coverage. 2) The public protein databases are often insufficient for searching non-human species because of the limited available genomic information. 3) The identification of the functions and biological processes of thousands of proteins is a formidable task because of the lack of simple and user-friendly software to automate gene ontology (GO) annotation. Furthermore it is

From the Departments of ‡Tumor Genetics and Biology and ¶Immunogenetics, Graduate School of Medical Sciences, Kumamoto University and §General Research Core Laboratory, Kumamoto University Medical School, 1-1-1 Honjo, Kumamoto 860-8556, Japan

Received, April 7, 2009, and in revised form, June 12, 2009
Published, MCP Papers in Press, June 13, 2009, DOI 10.1074/mcp.M900179-MCP200

[1] The abbreviations used are: iTRAQ, isobaric tagging for relative and absolute quantitation; NGF, nerve growth factor; GO, gene ontology; PC12PRS, PC12 proteome reference set; ICC, immunocytochemistry; siRNA, short interfering RNA; TCTP, translationally controlled tumor protein; ProTα, prothymosin α; TrkA, tropomyosin-related kinase A; 2-D, two-dimensional; RP, reverse phase; GOA, gene ontology annotation; PCNA, proliferating cell nuclear antigen; PI, propidium iodide; PAIRBP1, plasminogen activator inhibitor 1 RNA-binding protein; PAI, plasminogen activator inhibitor; mESC, mouse embryonic stem cell; MAGE, melanoma antigen; p75NTR, p75 neurotrophin receptor; QqTOF, quadrupole/quadrupole/time-of-flight mass spectrometers.

difficult to convert large lists of taxonomically diverse proteins into their human orthologs to obtain the richest GO information available. 4) Lastly biological validation strategies for identified proteins have not been standardized. Therefore, we believe an analysis framework that provides (*a*) comprehensive proteome data; (*b*) a simple and quick tool for organizing, enriching, and sorting those data to reveal candidate molecules for relation to certain processes; and (*c*) a standardized biological validation technique would greatly benefit this field. We therefore designed a concise, three-step, sequential proteomics strategy that addresses the above concerns and utilized it successfully in studying the mechanism of neuronal differentiation in PC12 cells.

PC12 cells (9) have been widely used as a model of neurons because of their unique advantages, such as stability, homogeneity, strong nerve growth factor (NGF) responsiveness, high differentiation potential, and a wealth of accessible background material, which help to facilitate their manipulation (10). This cell line has also been used for studying the mechanisms of neuronal disorders such as Alzheimer (11), Huntington (12), and Parkinson diseases (13) and neurofibromatosis type 1 (14–16). Here we used PC12 cells as a model for characterizing the mechanisms of neuronal differentiation and neurodegenerative disorders by means of MS-based quantitative proteomics.

NGF is one member of a family of structurally and functionally related dimeric polypeptides, neurotrophins, that are essential for the development and maintenance of distinct neuronal populations in the central and peripheral nervous systems (17). The initial signaling cascades in the neuronal cells right after NGF stimulation have been subjected to thorough investigation and characterization by using PC12 cells. After binding of extracellular NGF to the cell membrane-localized tropomyosin-related kinase A (TrkA) receptor, TrkA receptors dimerize and subsequently autophosphorylate each other. Then the phosphorylated receptors recruit a complex of signaling molecules and induce a number of intracellular signaling cascades involving the signaling molecules, such as phosphoinositide 3-kinase, phospholipase C-γ, and Ras (18). The posttranslational modifications, such as phosphorylation cascades, triggered by NGF stimulation play important roles in PC12 cell differentiation. However, knowledge of the precise dynamic molecular events of protein expression in response to NGF signaling in PC12 cells after an interval that allows the stimulation to take full effect and produce morphological changes remains far from complete.

Several reported studies have applied such methods as expressed sequence tag (19), restriction landmark cDNA scanning (20), targeted display (21), serial analysis of gene expression (22), and cDNA microarray (23) to survey the global change of differentially expressed genes in PC12 cells before and after NGF treatment (19–23). However, the genes and underlying mechanisms associated with the acquisition of a neuronal phenotype in these cells have not been clarified. Also a few proteomics approaches have been used for identifying the proteins related to NGF-inducible neurite formation in PC12 cells. For example, 2-D electrophoresis was applied in whole-cell extract separation to study the NGF modulation of protein synthesis (24); however, only two peptides were identified (25). Even currently available PC12 cell 2-D databases include merely a few proteins related to NGF stimulation (26–29). There is thus a paucity of functional proteomic information related to PC12 cell biological processes that may be attributed to technical limitations such as those listed above.

In this study, we performed the first proteomics survey of proteins differentially expressed in PC12 cells during NGF treatment by using a semiquantitative differential LC shotgun method, namely isobaric tagging for relative and absolute quantitation (iTRAQ) coupled with concurrent use of two tandem MS/MS systems, namely nano-LC-MALDI-TOF-TOF and nano-LC-ESI-Quadrupole/quadrupole/time-of-flight mass spectrometers. The total list of proteins identified was converted into a new file linked to the GO database by our proprietary GO analysis tool for proteomes (MANGO) and categorized by biological process and function using specific classification methods. Thereafter we classified the subset of proteins that were up- or down-regulated during neurite formation into specific molecular categories by combining the differential data obtained by iTRAQ with the proteomic GO analysis results. We then attempted to characterize the functional mechanism of NGF-induced PC12 cell neuronal differentiation. Interestingly the specific up-regulated groups classified in this study were related to apoptosis/cell survival in addition to cell motility, differentiation, stress stimulation, and morphogenesis. To investigate the molecular functions of the up-regulated proteins in relation to both PC12 cell differentiation and apoptosis/survival during neurite formation, some of them were further analyzed with a biochemical and cellular biological strategy using a combined antibody and siRNA technique. Lastly we demonstrated the advantages that our concise, sequential proteomics strategy offers for studying the molecular mechanisms of cellular biological events such as cell differentiation and survival/apoptosis.

EXPERIMENTAL PROCEDURES

Cell Culture, NGF Treatment, and Preparation of Cell Lysate—PC12 cells were cultured under 5% CO_2 at 37 °C in Dulbecco's modified Eagle's medium supplemented with 10% horse serum and 5% fetal bovine serum. We performed four independent cell cultures for a fourplex iTRAQ analysis. Two of them were used as duplicated samples for controls, and the other two samples were used as NGF-treated cells. For NGF stimulation, the cells were cultured onto collagen-coated culture dishes (Iwaki) in the same medium and stimulated with 50 ng/ml 2.5 S NGF (Wako) at 48 h. For preparation of cell lysate, cells were solubilized with the lysis buffer containing 8 M urea, 2% CHAPS, 2 mM Na_2VO_4, 10 mM NaF, 1 μM okadaic acid, and 1% (v/v) protease inhibitor mixture (Sigma) and passed through a 25-gauge syringe 15 times. Lysates were centrifuged at 13,000 × *g* for 20 min at 4 °C, and the protein concentration of the supernatants was determined using the Bio-Rad protein assay.

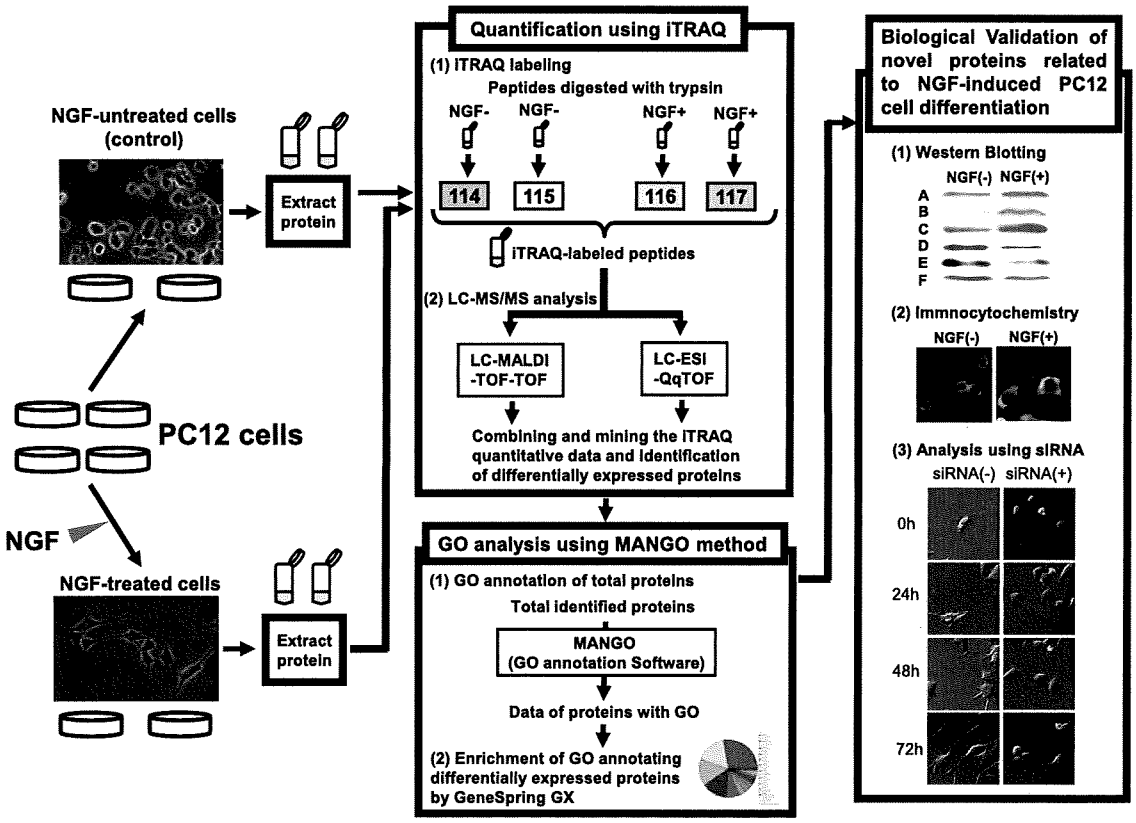

FIG. 1. **Work flow for the identification of the novel proteins regulating NGF-induced differentiation in PC12 cells.** For the fourplex iTRAQ labeling, the four lysates of PC12 cells separately cultured were prepared in parallel. The tryptic peptides from untreated cells and NGF-treated cells were labeled using mass 114/115 and 116/117 isobaric iTRAQ tags, respectively. These labeled peptides were analyzed with LC-MALDI-TOF-TOF or LC-ESI-QqTOF, and the quantification of each protein was performed according to the obtained iTRAQ data. Further biological and functional interpretation of the differentially expressed proteins was carried out by proteomics GO analysis using the MANGO method followed by cell biological analyses. Proteins *A–F* are candidates for novel molecules related to NGF-induced PC12 cell differentiation.

iTRAQ Sample Labeling—One hundred micrograms of each protein sample was precipitated using a 2-D Clean-Up kit (Amersham Biosciences), and the precipitants were dissolved in 10 μl of 6 M urea. iTRAQ sample labeling was performed according to the manufacturer's protocol with minimum modification. For the fourplex iTRAQ labeling, the four lysates of PC12 cells separately cultured were treated with iTRAQ reagents in parallel. Twenty microliters of dissolution buffer and 1 μl of denaturant reagent were added to the samples. The samples were reduced by addition of 2 μl of reducing reagent and incubation at 60 °C for 1 h. Reduced cysteine residues were then blocked by addition of 1 μl of cysteine blocking reagent and incubated at room temperature for a further 10 min. Tryptic digestion was initiated by the addition of 12.5 μl of trypsin solution (Promega; prepared as 1 μg/μl in water solution) and incubated at 37 °C for 16 h. To label the peptides with iTRAQ reagents, one vial of labeling reagent was thawed and reconstituted in 80 μl of ethanol. The reagents 114 and 115 for two samples from untreated cells and the reagents 116 and 117 for two samples from NGF-stimulated cells were added to the digests and incubated for 1 h at room temperature. The labeled samples were then mixed together before fractionation using a cation exchange column.

Sample Fractionation and Desalting—To remove excess, unbound iTRAQ reagent and to simplify the peptide mixture, the labeled peptide mixture was purified and fractionated using a GE Healthcare AKTA system. The mixed sample was diluted in loading buffer (20% (v/v) ACN and 10 mM potassium phosphate, pH 3.0) and loaded onto a Mono S column (GE Healthcare) equilibrated with loading buffer. Peptides were eluted with a gradient of solvent B (10 mM potassium phosphate, pH 3.0, and 1 M KCl in 20% (v/v) ACN) as follows: 0–2 min, 0–7% B; at 6 min, to 14% B; at 8 min, to 32% B; at 13 min, to 70% B; and at 21 min, to 100% B. Twenty-five fractions that included the iTRAQ-labeled peptides were used for analysis. The fractions were dried in a vacuum centrifuge and rehydrated with solution containing 2% ACN and 0.1% TFA. The samples were desalted with ZipTip™ μ-C_{18} pipette tips (Millipore). The desalted peptides were divided into two fractions to analyze the same samples by using nano-LC-MALDI-TOF-TOF and nano-LC-ESI-QqTOF systems.

LC-MALDI-MS/MS Analysis—Samples were separated by C_{18} nano-LC using DiNa Map (KYA Tech Corp.) equipped with a device spotting eluted fractions on a MALDI plate. Sample was injected onto a C_{18} column (0.5-mm inner diameter × 1-mm length, KYA Tech Corp.) equilibrated with solvent A (2% ACN and 0.1% TFA) and resolved on a C_{18} nanocolumn (0.15-mm inner diameter × 100-mm length; KYA Tech Corp.) at a flow rate of 300 nl/min with a 90-min gradient of solvent B (70% ACN and 0.1% TFA) as follows: 0–20% B from 0 to 10 min, to 50% B at 65 min, and to 100% B at 75 min. Column effluent was mixed with matrix (2 mg/ml α-cyano-4-hydroxycinnamic acid in 50% ACN and 0.1% TFA) at a flow rate of 1.4 μl/min.

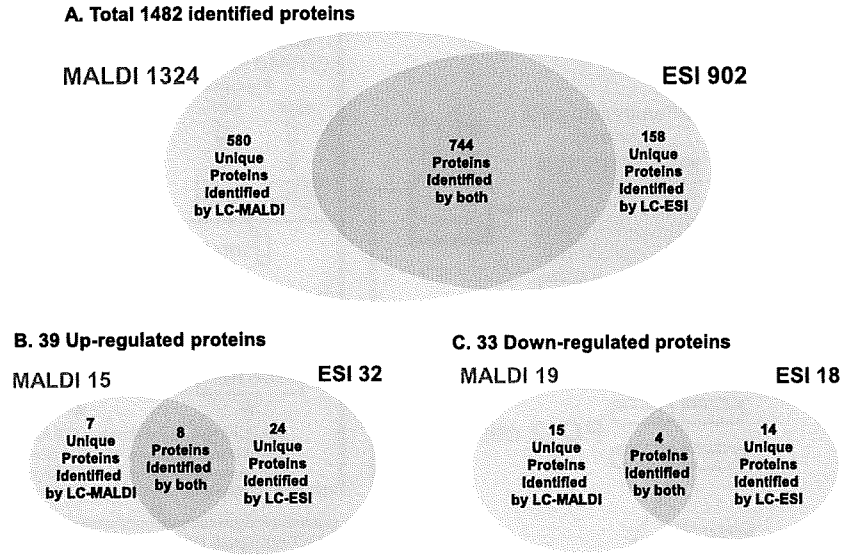

FIG. 2. **Venn diagrams of the number of total (*A*), up-regulated (*B*), and down-regulated (*C*) proteins identified by iTRAQ.** *A*, in total, 1,482 proteins of all taxonomies listed in supplemental Table 1 were identified with a confidence limit of 95%. *B* and *C*, for quantification of each protein identified by MALDI or ESI, a -fold change of each protein expression was calculated by comparing the average iTRAQ ratio of 116 and 117 as NGF-treated groups with the average ratio of 114 and 115 as control groups. Proteins quantified with a -fold change more than 20% (average iTRAQ ratio >1.20 or <0.83) and a p value less than 0.05 by MALDI or ESI were identified as differentially expressed proteins (*B* and *C*).

Fractions were spotted at 30-s intervals onto a stainless steel MALDI target plate (192 wells/plate; Applied Biosystems). Mass spectra of the peptides were acquired on a 4700 Proteomics Analyzer (Applied Biosystems) using 4000 Series Explorer software (Version 3.6). Mass spectra from *m/z* 800 to 4,000 were acquired for each fraction with 1,500 laser shots. To analyze the less abundant peptides, all of the peaks with a signal to noise ratio threshold from 50 to 75 and from 75 to 100 in each MS spectrum were selected for MS/MS analysis with 5,000 and 4,000 laser shots, respectively. Next all of the peaks above a signal to noise ratio threshold of 100 were selected for MS/MS analysis with 3,000 laser shots. Fragmentation of the labeled peptides was induced by the use of atmosphere as a collision gas with a pressure of 1×10^{-6} Torr and a collision energy of 1 kV.

LC-ESI-MS/MS Analysis—Samples were analyzed by nano-LC-ESI-MS/MS using the LC Packings Ultimate instrument fitted with a 20-μl sample loop. Samples were loaded onto a 5-mm RP C_{18} precolumn (LC Packings) at 30 μl/min and washed for 10 min before switching the precolumn in line with the separation column. The separation column used was a 75-μm internal diameter × 150-mm length PepMap RP column from LC Packings packed with 3-μm C_{18} beads with 100-Å pores. The flow rate used for separation on the RP column was 200 nl/min with a 90-min gradient of solvent B (85% ACN and 0.1% formic acid) as follows: 0–40% B from 0–60 min to 100% B at 70 min. The samples were divided into two fractions beforehand, and the first analysis was performed on a QSTAR Pulsar i mass spectrometer (Applied Biosystems/MDS Sciex), and the software used for data acquisition was Analyst QS 1.1 (Applied Biosystems/MDS Sciex) with the scan cycles set up to perform a 1-s MS scan followed by three MS/MS scans of the three most abundant peaks for 3 s each. Data acquisition was performed with an exclusion of 60 s for previous target ions. To analyze the less abundant peptides, the second analysis was performed under the same condition except for input of the *m/z* list to exclude the analyses of peptide ions already analyzed in the first run. The labeled peptides were fragmented under CID conditions designed to give iTRAQ reporter ions.

Data Analysis—Data from MALDI or ESI analysis were analyzed using the Paragon™ algorithm (30) of ProteinPilot Version 2.0 (Applied Biosystems), and the database searched was the Swiss-Prot database with all taxonomy (Revision number 53, 269,293 sequence entries, updated on May 29, 2007). Identified proteins were grouped by the Paragon algorithm of the software to minimize redundancy. This software has a function of automatic grouping of identified proteins according to the identified peptide sequence. The identified proteins were automatically grouping by the Paragon algorithm. Peptides used for the quantification of proteins were chosen by this algorithm of ProteinPilot software. All peptides used for the calculation of protein ratios were unique to the given protein or proteins within the group; peptides that were common to other isoforms or proteins of the same family that were reported separately were ignored. The ProteinPilot cutoff score used was 1.3, which corresponds to a confidence limit of 95%. The six user-defined options used included (i) cysteine alkylation, methyl methane thiosulfate; (ii) digestion, trypsin digestion; (iii) special factors, none; (iv) species, all species; (v) identification focus, biological modifications; and (vi) search effort, thorough identification search. For quantification of each protein identified in the MALDI or ESI analysis, a -fold change of each protein expression was calculated by comparing the average iTRAQ ratio of 116 and 117 as NGF-treated groups with the average ratio of 114 and 115 as control groups. Proteins quantified with a -fold change of more than 20% (average iTRAQ ratio >1.20 or <0.83) and a p value less than 0.05 (Student's t test) in the MALDI or ESI analysis were identified as differentially expressed proteins.

Proteomics GO Analysis by MANGO Method—To automate both the conversion of all identified proteins of multiple taxonomies into their human orthologs and annotation with GO information, a tool for taxonomy conversion/GO annotation, Molecular Annotation by Gene Ontology (MANGO), was designed as a Web-based application using the mySQL 4.0 database management system and scripts written in Java. Ensembl Mart and UniProt GOA (GOA UniProt Version 49.0, June 2007 update) files were integrated into the database and were used as the external reference data for the taxonomy conversion and the GO annotation, respectively. For the proteins that could not be automatically converted to the human orthologs using this conversion/annotation tool, we searched the human orthologs by using National Center for Biotechnology Information basic local alignment search tool (NCBI BLAST) programs. A list of 1,404 human GO-annotated proteins was compiled and was designated as the PC12 proteome reference set for analysis with GeneSpring GX (supplemental Table 4). GeneSpring GX Version 7.3.1 was used to determine the GO categories that were statistically overrepresented in the iTRAQ data set. GO categories, by which at least three proteins were annotated, were accepted at the significance level of $p < 0.05$ (Fisher's

TABLE I

List of proteins differentially-expressed in response to NGF stimulation

snRNA, small nuclear RNA; —, not applicable.

Protein name abbreviation	Protein name	Accession no.	Theoretical molecular mass (kDa)/pI	MALDI		ESI		Ref.[b]
				Average ratio[a]	*p* value	Average ratio[a]	*p* value	
Up-regulated proteins								
VGF	Neurosecretory protein VGF	P20156	68.2/4.7	**2.935**	0.011	**3.770**	0.024	23, 40
NEUM	Neuromodulin	P07936	23.6/4.6	**1.791**	0.008	**2.936**	0.021	23, 41
MOES	Moesin	O35763	67.7/6.2	**1.691**	0.035	**1.679**	0.030	—
CMGA	Chromogranin A	P10354	52.0/4.7	**1.594**	0.003	**1.596**	0.003	42
ANXA2	Annexin A2	Q07936	38.7/7.6	**1.449**	0.048	**1.805**	0.037	23, 43
PERI	Peripherin	P21807	53.5/5.4	**1.329**	0.011	**1.429**	0.012	44
AT1A1	Sodium/potassium-transporting ATPase α-1 chain	P06685	11.3/5.3	**1.271**	0.048	**1.341**	0.003	23
MAP1B	Microtubule-associated protein 1B	P15205	269.5/4.7	**1.250**	0.010	**1.352**	0.027	45
SQSTM	Sequestosome-1	O08623	47.7/5.1	**1.764**	0.042			—
RIR2	Ribonucleoside-diphosphate reductase M2 subunit	Q4KLN6	45.0/5.5	**1.339**	0.044			—
SGTA	Small glutamine-rich tetratricopeptide repeat-containing protein A	O70593	34.2/5.1	**1.286**	0.035	1.051	0.787	—
CROP	Cisplatin resistance-associated overexpressed protein	O95232[c]	51.5/9.8	**1.266**	0.042	1.006	0.294	—
PAIRBP1	Plasminogen activator inhibitor 1 RNA-binding protein	Q6AXS5	44.8/8.6	**1.226**	0.013	1.241	0.113	—
GSPT1	G_1 to S phase transition protein 1 homolog	P15170[c]	55.8/5.5	**1.206**	0.042	0.977	0.841	—
CRIP2	Cysteine-rich protein 2	P36201	22.7/8.9	**1.205**	0.020			—
PROTA	Prothymosin α	P06302	12.4/3.8	1.642	0.206	**2.173**	0.037	—
AHNAK	Neuroblast differentiation-associated protein AHNAK	Q09666[c]	629.1/5.8	1.245	0.113	**1.947**	0.012	46
SCG2	Secretogranin-2	P10362	71.0/4.7	1.339	0.068	**1.633**	0.027	42
AT1B1	Sodium/potassium-transporting ATPase subunit β-1	P07340	35.2/8.8	1.423	0.062	**1.630**	0.001	23
MAGED1	Melanoma-associated antigen D1	Q9ES73	85.8/7.1	1.066	0.654	**1.630**	0.020	—
LEG1	Galectin-1	P11762	14.9/5.1	1.272	0.126	**1.578**	0.016	22, 23
ENPL	Endoplasmin	P14625[c]	92.5/4.8	1.052	0.134	**1.556**	0.016	22, 23
S100A6	Protein S100-A6	P05964	10.0/5.3	1.362	0.069	**1.552**	0.004	—
E2IG5	E2-induced gene 5 protein homolog	Q4QQV3	17.8/10.0	1.240	0.103	**1.547**	0.023	23
CRMP4	Dihydropyrimidinase-related protein 3 (CRMP4)	Q62952	62.0/6.0	1.183	0.240	**1.407**	0.016	23
SRRM2	Serine/arginine repetitive matrix protein 2	Q8BTI8[d]	294.7/12.0	0.981	0.667	**1.377**	0.013	—
DNJA1	DnaJ homolog subfamily A member 1	P63036	44.9/6.7	1.065	0.397	**1.331**	0.011	—
RAC1	Ras-related C3 botulinum toxin substrate 1	Q6RUV5	21.5/8.8			**1.316**	0.044	—
TCTP	Translationally controlled tumor protein	P63029	19.5/4.8	1.359	0.126	**1.291**	0.016	—
RAB2A	Ras-related protein Rab-2A	P05712	23.5/6.1	1.272	0.239	**1.280**	0.015	—
OXRP	Hypoxia up-regulated protein 1	Q63617	111.3/5.1	1.051	0.591	**1.271**	0.008	—
PRDX6	Peroxiredoxin-6	O35244	24.8/5.6	1.128	0.207	**1.268**	0.008	—
ENOA	α-Enolase	P04764	47.1/6.2	1.153	0.172	**1.253**	0.008	23
RADI	Radixin	P35241[c]	68.6/6.0	0.885	0.193	**1.251**	0.032	23
ALDR	Aldose reductase	P07943	35.8/6.3	1.276	0.235	**1.248**	0.004	—
PDI	Protein-disulfide isomerase	P04785	57.0/4.8	1.041	0.118	**1.245**	0.045	23
FABPE	Fatty acid-binding protein, epidermal	P55053	15.1/6.73	1.136	0.268	**1.227**	0.049	23
RGP1	Ran GTPase-activating protein 1	P46061[d]	63.6/4.6	1.027	0.359	**1.219**	0.012	—
NUCB1	Nucleobindin-1	Q63083	53.5/5.0	1.039	0.521	**1.208**	0.005	—
Down-regulated proteins								
K1C18	Keratin, type I cytoskeletal 18	Q5BJY9	47.8/5.2	**0.626**	0.028	**0.566**	0.043	—
K2C8	Keratin, type II cytoskeletal 8	Q10758	54.0/5.8	**0.690**	0.011	**0.599**	0.040	—
PRPS2	Ribose-phosphate pyrophosphokinase II	P09330	34.8/6.2	**0.690**	0.040	**0.642**	0.015	—
LDHA	L-Lactate dehydrogenase A chain	P04642	36.5/8.5	**0.768**	0.022	**0.792**	0.041	—
PRP19	Pre-mRNA-processing factor 19	Q9JMJ4	55.2/6.2	**0.551**	0.009	0.880	0.604	—
VTDB	Vitamin D-binding protein	P04276	53.5/5.7	**0.625**	0.006			—
IDHP	Isocitrate dehydrogenase (NADP), mitochondrial	P56574	51.0/8.9	**0.630**	0.005	0.868	0.068	—
HNRLL	Heterogeneous nuclear ribonucleoprotein L-like	Q921F4[d]	64.1/5.8	**0.651**	0.031	0.636	0.187	—
NUCKS	Nuclear ubiquitous casein and cyclin-dependent kinase substrate	Q9EPJ0	27.1/5.0	**0.747**	0.006			—
API5	Apoptosis inhibitor 5	Q9BZZ5[c]	57.6/5.8	**0.748**	0.013	0.777	0.116	—
H2B1C	Histone H2B type 1	Q00715	14.0/10.4	**0.762**	0.040	0.860	0.003	23
RL34	60 S ribosomal protein L34	P11250	13.5/11.7	**0.769**	0.049			—
RLA0	60 S acidic ribosomal protein P0	P19945	34.2/5.9	**0.772**	0.035	0.962	0.605	—
TBB4	Tubulin β-4 chain	P04350[c]	49.6/4.8	**0.784**	0.034			—
SRR35	35-kDa SR repressor protein	Q8WXF0[c]	30.5/11.7	**0.787**	0.001			—
PCNA	Proliferating cell nuclear antigen	P04961	28.7/4.6	**0.790**	0.043	0.743	0.060	—

TABLE I—*continued*

Protein name abbreviation	Protein name	Accession no.	Theoretical molecular mass (kDa)/pI	MALDI		ESI		Ref.[b]
				Average ratio[a]	*p* value	Average ratio[a]	*p* value	
UBP48	Ubiquitin carboxyl-terminal hydrolase 48	Q76LT8	118.8/5.9	**0.793**	0.016			—
GSTM2	Glutathione *S*-transferase Mu 2	P08010	25.7/6.9	**0.794**	0.024	0.825	0.055	23
CB39L	Calcium-binding protein 39-like	Q9H9S4[c]	39.1/8.5	**0.818**	0.033			—
LSM8	U6 snRNA-associated Sm-like protein LSm8	O95777[c]	10.4/4.4			**0.648**	0.015	—
DDC	Aromatic-L-amino-acid decarboxylase	P14173	54.1/6.5			**0.669**	0.045	23
CSK21	Casein kinase II subunit α	P19139	45.1/7.3	0.875	0.088	**0.670**	0.041	—
RL6	60 S ribosomal protein L6	P21533	33.6/10.7	0.904	0.497	**0.681**	0.040	—
GALK1	Galactokinase	Q9R0N0[d]	42.2/5.2	1.222	0.509	**0.730**	0.029	—
AB14B	Abhydrolase domain-containing protein 14B	Q8VCR7[d]	22.5/5.8	0.675	0.292	**0.748**	0.030	—
HNRPF	Heterogeneous nuclear ribonucleoprotein F	Q794E4	45.7/5.3	1.053	0.294	**0.756**	0.031	—
APT	Adenine phosphoribosyltransferase	P36972	19.5/6.2	0.942	0.724	**0.783**	0.028	—
H2A2B	Histone H2A type 2-B	Q8IUE6[c]	14.0/10.9	0.860	0.157	**0.814**	0.024	23
FUBP2	Far upstream element-binding protein 2	Q99PF5	74.2/6.4	0.949	0.090	**0.818**	0.002	—
FINC	Fibronectin	P04937	272.5/5.5	0.688	0.172	**0.819**	0.000	—
TIM13	Mitochondrial import inner membrane translocase subunit Tim13	P62076	10.5/8.4	1.003	0.974	**0.820**	0.025	—
SFRS2	Splicing factor, arginine/serine-rich 2	Q6PDU1	25.5/11.9	0.852	0.249	**0.826**	0.005	—
FEN1	Flap endonuclease 1	P39748[c]	42.6/8.8	0.971	0.775	**0.833**	0.022	23

[a] The average ratio of iTRAQ data with *p* value smaller than 0.05 is highlighted with bold font.
[b] The proteins with Refs. 22 and 23 had been reported previously as NGF-responsive genes at the mRNA level.
[c] Proteins identified with human taxonomy.
[d] Proteins identified with mouse taxonomy.

exact test). The annotation data of the 72 differentially expressed proteins were used to determine the overrepresented biological processes related to NGF-induced PC12 cell differentiation. A GO tree view composed of enriched biological processes in the up-regulated proteins was built according to the tree view in AmiGO, a tool for searching and browsing the Gene Ontology database (31).

Western Blotting—Cell lysate samples containing 20 μg of total protein were electrophoresed on SDS-polyacrylamide gels, transferred onto a PVDF membrane by electroblotting, and subjected to immunoblotting with the indicated antibody. In the case of prothymosin α (ProTα), cell lysate samples were transferred onto a membrane by electroblotting with acidic buffer (20 mM sodium acetate buffer, pH 5.2) followed by fixation with 0.5% glutaraldehyde (32, 33). Membranes were probed with different primary antibodies followed by horseradish peroxidase-conjugated mouse, rabbit, and goat secondary antibodies (GE Healthcare). The images were visualized with ECL (GE Healthcare). The following primary antibodies were used: neurosecretory protein VGF, CRMP-4, galectin-1, ProTα, MAGED1, and PCNA (Santa Cruz Biotechnology); plasminogen activator inhibitor 1 RNA-binding protein (PAIRBP1) (Abnova Co.); translationally controlled tumor protein (TCTP) (MBL International Corp.); β-actin (Sigma); peroxiredoxin 6 (Lab Frontier); and protein-disulfide isomerase (Stressgen). For the quantitative analysis, the ECL patterns were scanned using LabScan 5.0 (GE Healthcare) with transparent mode and a resolution of 300 dpi. The intensities were measured using ProGenesis Workstation Version 2005 (PerkinElmer Life Sciences).

Transfection of PC12 Cells with siRNA—Transfection of PC12 cells with siRNA was performed using Lipofectamine 2000 (Invitrogen) according to the manufacturer's protocol. Four target sequences for rat, PAIRBP1, TCTP, ProTα, and MAGED1 siRNA, were designed as follows. A 21-oligonucleotide siRNA duplex was designed as recommended elsewhere and was synthesized by Gene Link to target the PAIRBP1 sequence (5′-^{1125}AAGUGCUUCUGCUCCUGACTT-3′), the TCTP sequence (5′-^{357}AAGCACATCCTTGCTAATTTT-3′), the ProTα sequence (5′-52AAGGAGAAGAAGGAAGUUGTT-3′), and the MAGED1 sequence (5′-^{1928}AAGUGCUGAGAUUCAUUGCTT-3′). A Silencer Negative Control siRNA 1 (Ambion) was used as a control siRNA for the analysis.

Immunofluorescence Analysis—PC12 cells cultured on 35-mm collagen-coated culture dishes were fixed with 4% paraformaldehyde in PBS for 15 min at room temperature and then permeabilized with 0.1% Triton X-100 in PBS on ice for 15 min. After being washed with PBS, cells were incubated in primary antibodies diluted in PBS containing 5% bovine serum albumin followed by anti-mouse or -rabbit Alexa Fluor® 488-conjugated IgG (Invitrogen) for 60 min at room temperature. After being washed with PBS, the cells were incubated for 10 min at room temperature with rhodamine-phalloidin (Invitrogen) to stain cellular F-actin. After being washed with PBS, the cells were incubated for 10 min at room temperature with 20 μg/ml Hoechst33342 (Invitrogen) to stain nuclear actin. Analysis was performed with a fluorescence microscope (with 20 × 1.6 Olympus IX71) (DPController, DPManager).

Quantification of Neurite Outgrowth—For quantification of the neurite outgrowth of PC12 cells, the cells transfected with siRNAs were cultured onto collagen-coated culture dishes (Iwaki) under the condition of 1% horse serum and stimulated with 50 ng/ml 2.5 S NGF (Wako) at 48 h. Total neurite length of NGF-stimulated PC12 cells was measured using MetaMorph software (Molecular Devices). The total number of tip ends was manually counted to represent the number of neurites from individual cells. For each measurement, at least 50 cells per dish were analyzed from randomly selected fields. Each experiment was repeated three times.

Evaluation of PC12 Cell Death—Propidium iodide (PI) was used for the evaluation of PC12 cell death. Cells transfected with siRNAs were cultured onto 35-mm collagen-coated culture dishes (Iwaki) under the condition of 10% horse serum and 5% fetal bovine serum and stimulated with 50 ng/ml 2.5 S NGF (Wako) at 48 h. The cells were fixed with 4% paraformaldehyde in PBS and incubated with 0.2 μg/ml PI for apoptotic cells and 20 μg/ml Hoechst33342 (Invitrogen) for total cells for 10 min at room temperature. PI-positive cells were counted using a fluorescence microscope (with 20 × 1.6 Olympus IX71) (DPController, DPManager). For each counting, at least 500 cells per dish were counted from randomly selected fields. Each experiment was repeated three times.

Time Lapse Video Analysis—Cells were cultured on a collagen-coated glass bottom plate with 6 wells (Iwaki). The plate was main-